Peer reviewed version

License (if available):
CC BY

Link to published version (if available):
10.1016/j.kint.2019.09.035

Link to publication record in Explore Bristol Research
PDF-document

University of Bristol - Explore Bristol Research
General rights

Title page

Blocking matrix metalloproteinase-mediated syndecan-4 shedding restores the endothelial glycocalyx and glomerular filtration barrier function in early diabetic kidney disease

Raina D. Ramnath[1], Matthew J. Butler[1], Georgina Newman[1], Sara Desideri[1], Amy Russell[1], Abigail C. Lay[1], Chris R. Neal[1], Yan Qiu[1], Sarah Fawaz[1], Karen L. Onions[1], Monica Gamez[1], Michael Crompton[1], Chris Michie[1], Natalie Finch[1], Richard J Coward[1], Gavin I. Welsh[1], Rebecca R. Foster[1], Simon C. Satchell[1].

[1] Bristol Renal, Translational Health Sciences, Bristol Medical School, University of Bristol, Bristol, UK

Author for correspondence: Dr Raina Ramnath, Bristol Renal, Translational Health Sciences, Bristol Medical School, University of Bristol, Dorothy Hodgkin Building, Whitson Street, Bristol BS1 3NY, UK; Fax number: 0117 331 30 35; Tel number: 01173313106; Email: mdrdr@bristol.ac.uk

Running title: Syndecan 4 in diabetic kidney disease

Abstract

The endothelial glycocalyx is a key component of the glomerular filtration barrier. We have shown that matrix metalloproteinase (MMP)-mediated syndecan 4 shedding is a mechanism of glomerular endothelial glycocalyx damage *in vitro*, resulting in increased albumin permeability. Here we sought to determine whether this mechanism is important in diabetes *in vivo*. We studied early diabetic kidney disease in streptozotocin-induced type 1 diabetes in DBA2/J mice. Diabetic mice were albuminuric and had increased glomerular albumin permeability and endothelial glycocalyx damage. Syndecan 4 mRNA expression was upregulated in isolated glomeruli and flow cytometry-sorted glomerular endothelial cells. In contrast, glomerular endothelial luminal surface syndecan 4 and Marasmium oreades agglutinin lectin labelling measurements were reduced in diabetes. Similarly, syndecan 4 protein expression was significantly decreased in isolated glomeruli and increased in plasma and urine, suggesting syndecan 4 shedding. MMP 2, 9 and 14 mRNA expression were upregulated in isolated glomeruli, suggesting a possible mechanism of glycocalyx damage and albuminuria. We therefore characterised in detail the activity of MMP 2 and 9 and showed significant increases in kidney cortex, plasma and urine. Therapeutic treatment with MMP 2/9 inhibitor I at 5mg/kg/day for 21 days, started 6 weeks after diabetes induction, restored endothelial glycocalyx depth and coverage and attenuated diabetes-induced albuminuria and reduced glomerular albumin permeability. MMP inhibitor treatment significantly attenuated glomerular endothelial and plasma syndecan 4 shedding and inhibited plasma MMP activity. These studies confirm the importance of MMPs in endothelial glycocalyx damage and albuminuria in early diabetes and demonstrate that this pathway is amenable to therapeutic intervention. Treatments targeted at glycocalyx protection by MMP inhibition may be of benefit in diabetic kidney disease.

Translational Statement

Manipulating glycocalyx, through MMP inhibition, provides an attractive therapeutic target in diabetic kidney disease. MMP inhibitor treatment is realistic in the clinical setting: tetracyclines, an antibiotic agents, inhibit MMPs at sub-antibiotic doses and have been shown to have benefits in human disease[1, 2] and low dose doxycycline (MMP inhibitor) is licensed for the treatment of periodontitis.[3] The development of more specific MMP inhibitors promises to reduce the adverse effects associated with broad-spectrum MMP inhibitors seen in some clinical trials. Shed glycocalyx components including SDC4 warrant further investigation as potential biomarkers for diabetic kidney disease and associated cardiovascular complications.

Keywords

Glomerular endothelial glycocalyx, diabetes, syndecan 4, matrix metalloproteinase

Introduction

Diabetic kidney disease (DKD) is a serious complication of diabetes developing in approximately 1 in 3 people with diabetes. The cost of treating diabetic complications, including DKD, is expected to rise from the current total of £7.7 billion to £13.5 billion by 2035/6 in the UK.[4] Despite this, renin-angiotensin system blockade remains the only established treatment in slowing the progression of disease and delaying renal failure. New treatments specifically targeting key steps in disease evolution are desperately needed.

The glomerular endothelium is emerging as a key player in diabetes and other glomerular diseases.[5] The glomerular endothelial cell (GEnC) glycocalyx in particular plays an important role in glomerular barrier function.[6, 7] The endothelial glycocalyx is a hydrated poly-anionic gel present on the luminal surface of all endothelial cells and is composed principally of proteoglycans.[8] Proteoglycans consist of a core protein, e.g. a syndecan (SDC) and

glycosaminoglycan (GAG) side chains, e.g. heparan sulphate (HS). SDC1 and 4 in particular are prominent in the kidney.[9-12] SDC4 has a short cytoplasmic domain and an ectodomain which carries 3-5 HS chains,[13-15] and is the most abundant amongst the SDC family in human GEnC.[16]

Endothelial glycocalyx has multiple roles in vascular homeostasis[17] and its disruption contributes to several vascular diseases including diabetes.[6-8, 18] Our group and others have shown that the glomerular endothelial glycocalyx contributes to the barrier to albumin permeability in cultured cells[18-20] and *in vivo*.[21-24] Loss of GAG within the glomerular capillary wall is seen in albuminuric diabetic rats[25] and diabetic mice.[26, 27] In humans systemic glycocalyx dimensions are reduced in diabetes.[28, 29] Loss of systemic and glomerular glycocalyx is associated with the development of microalbuminuria in diabetes, suggesting that glycocalyx dysfunction contributes to the pathogenesis of this condition.[6, 30]

Glycocalyx components are cleaved from the cell surface by 'sheddases' including matrix metalloproteinases (MMPs).[13, 16] Gelatinases MMP2 and 9 can be activated by membrane type 1 MMP, also known as MMP14. We and others have shown that diabetic conditions induce upregulation of endothelial MMP9,[16] MMP2[29] and urinary MMP14[31]; their enzymatic activities are elevated in diabetic human[31, 32] and mouse[33] kidneys. The dysregulation of MMP 2 and 9 activities has been associated in the pathophysiology of several diabetic co-morbidities.[34-36] Urinary MMP2 and 9 concentration and activity are increased in type 1 diabetic patients with albuminuria.[36-38]

We have previously shown that in response to TNFα, an inflammatory mediator which is increased in diabetic milieu, SDC4 was specifically and significantly upregulated amongst other SDCs in human GEnC *in vitro*.[16] TNFα treatment caused a disruption of the GEnC glycocalyx through MMP9-mediated shedding of SDC4 and HS and this was accompanied

by an increase in protein permeability across GEnC monolayers.[16] Here we seek to determine whether this mechanism is important in glomerular disease in diabetes *in vivo*. We hypothesise that GEnC glycocalyx dysfunction in diabetes is caused by MMP-mediated shedding of SDC4 and that this is amenable to therapeutic intervention.

Results

Glomerular endothelial glycocalyx damage accompanies albuminuria in early DKD

DBA/2J mice became hyperglycemic 2 weeks after the first of five daily STZ injections (Fig. 1 Ai). There was no significant change in body weight in the STZ-treated mice when compared to baseline, prior to STZ injection (Fig. 1 Aii). However, the diabetic mice gained less weight than control mice, resulting in a 1.2-fold lower body weight after week 8 post STZ (Fig. 1 Aii). The mice became significantly albuminuric after week 6 post STZ, and this persisted until the mice were culled with a 4.9-fold increase in albuminuria (Fig. 1Bi) at 8 week post STZ. Compromised glomerular capillary wall integrity was confirmed by a 2-fold increase in glomerular albumin permeability (Ps'alb) (Fig. 1Bii). Permeability changes were associated with disruption of the glomerular glycocalyx. There was a 2-fold decrease in endothelial glycocalyx depth measured by electron microscopy but no significant change in glycocalyx coverage (Fig. 1C, D). Moreover, a decrease in podocyte glycocalyx depth was observed but no significant change in other ultrastructural features including glomerular basement membrane (GBM) thickness, slit diaphragm and foot process width (Supplementary Fig. 1A-E). Moreover, Picrosirius red staining showed no significant collagen deposition in diabetes when compared to control (Supplementary Fig. 1F-G), confirming the electron microscopy results, suggesting no change in GBM structure. Marasmium oreades agglutinin (MOA) lectin bound specifically to the endothelial glycocalyx, on the luminal surface of the GEnC (determined using the membrane label R18) (Fig. 1Ei). We have applied our peak to peak measurement technique, previously used in

vivo,[39, 40] for the first time on fixed kidney tissue (Figure 1 Eii). Peak to peak measurement of MOA labelling, an index of glycocalyx thickness, demonstrated a 1.5 fold reduction in endothelial glycocalyx thickness in diabetes which is consistent with the reduction in endothelial glycocalyx depth observed by electron microscopy (Figure 1 Eiii).

Glycocalyx-related gene expression is modified in early DKD

Expression of the glomerular glycocalyx-related genes SDCs and glycocalyx modifying genes MMPs relative to glyceraldehyde-3-phosphate dehydrogenase (GAPDH) in untreated mice was determined. SDC4 mRNA expression was significantly higher than other SDC and MMP mRNAs (Fig. 2A), in line with SDC expression in human GEnC.[16] The effect of diabetes on the expression of different components of the glycocalyx was investigated in isolated glomeruli using a custom-designed TaqMan qPCR array focused on glycocalyx-related genes (Fig 2B, Supplementary Table 1) similar to that used previously.[16] Expression Suite software and $2^{-\Delta\Delta CT}$ method followed by *t*-test were used to analyse the array data and both methods showed a significant increase in SDC1, 4 and MMP14 mRNA expression amongst other significantly modulated gene expression (Fig 2B, Supplementary Table 2). SDC1, 3, 4 and MMP 14 were independently validated by real time qPCR demonstrating significant upregulation in all of them (Fig. 2C). Although there was no significant increase in MMP2 and 9 mRNA expression with the TaqMan qPCR array, because of previous data suggesting their importance they were further examined by individual qPCR which showed significant increase in MMP 2 and 9 (Fig. 2C). In contrast SDC2 was significantly downregulated (Fig. 2C).

SDC4 mRNA, protein and MMP activity are altered in early DKD

Expression of SDC4 and 1 mRNA specifically in GEnC was determined in cells isolated by flow cytometry (Supplementary, Fig 2). SDC4 mRNA expression was upregulated 2.5-fold (Fig. 3A) whereas SDC1 mRNA expression was not significantly changed in diabetes (Fig.

3B). To quantify endothelial glycocalyx SDC4 protein expression, an anti-SDC4 antibody was injected intravenously and shown to localise predominantly to GEnC (Supplementary, Fig 3). To specifically quantify the SDC4 on the luminal surface of the endothelial cells, we have used R18 labelling to highlight the endothelial membrane and enable separation of luminal from non-luminal labelling. Peak to peak measurement demonstrated a 2.8-fold reduction in glomerular endothelial glycocalyx SDC4 in diabetes (Fig. 3C). Similarly, SDC4 expression by ELISA was reduced 1.6-fold in diabetic glomeruli, suggesting glomerular SDC4 shedding (Fig. 3D), whereas SDC1 glomerular protein expression was not changed in diabetes (Fig. 3E). There was a 1.8-fold (Fig. 3F) and a 11.8-fold (Fig. 3G) increase in plasma and urine SDC4 concentration respectively, again consistent with systemic SDC4 shedding in diabetes. We measured the sheddases MMP2 and 9 and found that active MMP2 concentration was increased by 2-fold in kidney cortex lysate, 1.5-fold in plasma and 3-fold in urine (Fig. 4A-C) and active MMP9 concentration was increased by 1.8-fold in kidney cortex lysate, 1.8-fold in plasma and 2.5-fold in urine (Fig 4D-F).

MMP2 and 9 mediate disruption of the glomerular endothelial glycocalyx in early DKD
An MMP 2/9 inhibitor (MMPI) was given therapeutically, after the onset of albuminuria at week 6 post STZ, for 21 days (Fig. 5A). Blockade of MMP had no significant effect on glycaemia and body weight (Fig. 5B, C) but significantly attenuated the diabetes-induced increase in urinary albumin creatinine ratio by 2.6-fold (Fig. 5D). MMPI treatment reduced the diabetes-mediated increase in Ps'alb by 2-fold, restoring the permeability barrier of the glomerular capillaries (Fig. 5E). MMPI also restored diabetes-induced endothelial glycocalyx loss, evidenced by a 1.6-fold increase in endothelial glycocalyx depth and a 2-fold increase in endothelial glycocalyx coverage (Fig. 5F, G). MMPI treatment also resulted in a significant increase in podocyte glycocalyx depth, but there was no significant effect on GBM thickness, nor podocyte foot process and slit diaphragm width (supplementary Fig 3A-E).

Blockade of MMP2 and 9 ameliorates diabetes-induced changes in SDC4 and reduces plasma MMP activity

MMPI treatment restored the decrease in SDC4 labelling by peak to peak measurement 2.2-fold (Fig. 6A). It attenuated the increase in SDC4 mRNA expression observed in diabetes by 1.5-fold (Fig. 6B) and restored the loss of glomerular SDC4 protein expression by 1.8-fold (Fig. 6C). MMPI significantly attenuated diabetes-induced plasma SDC4 shedding by 2-fold but not urine SDC4 shedding (Fig. 6D, E). Therapeutic treatment with MMPI blocked diabetes-induced increase in plasma MMP2 and 9 activities by 2-fold and 1.2-fold respectively (Fig. 6F, G), confirming that this inhibitor reduces the activity of both MMPs in vivo.

Discussion

In this study, we investigated our hypothesis that GEnC glycocalyx dysfunction in diabetes is caused by MMP mediated SDC4 shedding and importantly, that is amenable to therapeutic intervention. We have used a model of early DKD, week 8-9 post STZ, resulting in the mice being hyperglycaemic and albuminuric. Due to tubular reabsorption of filtered albumin and changes in local hemodynamics, albuminuria is not a sensitive measure of glomerular permeability. Therefore, we have used our reliable, physiologically relevant glomerular albumin permeability assay to directly measure glomerular permeability using single capillaries in isolated glomeruli. The assay has been extensively validated and provided robust, reproducible estimates of glomerular albumin permeability.[24] We observed an increase in glomerular albumin permeability, confirming reduced glomerular capillary wall integrity in early DKD. The increase in albuminuria and in glomerular permeability was associated with a reduction in endothelial and podocyte glycocalyx depth without affecting other glomerular ultrastructure such as GBM thickness, podocyte slit diaphragm and foot process width. Moreover, there was no change in collagen deposition in our model using

Picrosirius red staining, this supports the electron microscopy data. Our findings are consistent with our previous work showing that at 8 weeks post STZ injection, type 1 diabetic mice do not develop GBM thickness and podocyte effacement.[41] GBM thickening has been reported in some but not all mouse models of diabetic nephropathy.[42] For example, GBM thickening occurs in diabetic DBA2J mice after ~25 weeks of hyperglycemia.[43] Our data confirms previous observations that loss of glomerular glycocalyx, in the absence of changes in other glomerular capillary wall components, is associated with albuminuria and glomerular permeability in early DKD.[24, 27]

The role of the podocyte glycocalyx has not previously been examined in detail so further work is necessary to determine the significance of our observation of podocyte glycocalyx loss in diabetes. Some studies support the hypothesis that endothelial activation can lead to secondary podocyte injury.[44-47] It has been shown that damage specifically to the glomerular endothelial glycocalyx using hyaluronidase results in extensive uptake of albumin by podocytes, which could initiate an inflammatory reaction resulting in podocyte damage.[48, 49] In this study, we observed endothelial and podocyte glycocalyx damage, however the damage to podocytes was not severe enough to cause foot process effacement in this model of early DKD.

MOA lectin, known to bind to specific carbohydrate sequences present in the glycocalyx of mouse glomerular endothelium,[50, 51] was used to specifically study the glomerular endothelial glycocalyx. Consistent with previous findings,[50, 51] MOA lectin localised to the glomerular endothelial glycocalyx; and our peak to peak measurement technique,[39, 40] demonstrated a reduction in endothelial glycocalyx thickness in diabetes, which complements and supports the electron microscopy data. The peak to peak measurement using MOA lectin labelling is greater than the glycocalyx thickness by electron microscopy. This is likely to be due to

endothelial glycocalyx collapse with the dehydration procedure that follows fixation in preparation for electron microscopy.[52]

The glycocalyx is a complex structure and which components are damaged in diabetes has not been previously defined. We show here that in untreated control mice, SDC4 mRNA was highly expressed in isolated glomeruli, which is in line with the SDC4 mRNA expression in human ciGEnC.[16] Custom designed qPCR array focusing on glycocalyx-related genes was used to determine the effect of diabetes on glomerular glycocalyx components. Proteoglycan SDC1 and 4 mRNA expression were considerably upregulated in isolated glomeruli in DKD. This is consistent with another study showing a 26-fold increase in renal/glomerular SDC4 mRNA in proteinuric DKD.[53] Furthermore, by using fluorescence activated cell sorted (FACS) mouse GEnC, we were able to show that SDC4 mRNA expression was specifically upregulated in this cell type. Our previous work on cultured human GEnC indicate that this SDC4 mRNA upregulation is a compensatory response to SDC4 shedding.[16] Indeed in line with the MOA lectin results, we showed a reduction in glomerular endothelial SDC4 peak to peak measurement in DKD. Similarly, glomerular glycocalyx SDC4 protein expression was considerably reduced in DKD, suggesting shedding of glomerular endothelial glycocalyx SDC4. This was also accompanied by an increase in plasma and urine SDC4 suggesting systemic glycocalyx shedding. Other glycocalyx components, including SDC1 concentration, have already been reported to be increased in serum from subjects with type 1 diabetes mellitus and microalbuminuria.[54] SDC4 is unlikely to be the only constituent that is being shed from the glycocalyx in diabetes. SDC4 carries HS side chains so HS shedding is likely to accompany SDC4 shedding as we have shown previously in vitro[16] and others have shown in vivo in a diabetes model.[55] Glycocalyx component hyaluronan[56] has also been shown to be shed in diabetes.

We then determined the underlying mechanism of SDC4 shedding in DKD. MMP2 and 9 are known to increase in human type 1 and type 2 diabetes[57-60] and their levels are altered in animal DKD models.[31, 32, 38, 60] In this study, we characterised in detail expression of relevant sheddases in different compartments and showed that MMP2 and 9 were upregulated at the mRNA level and their activities were enhanced in kidney cortex, plasma and urine in DKD. We also observed an increase in MMP14 mRNA expression in DKD, which was not surprising considering MMP14 is a known gelatinase activator.[61] The increase in MMP activity was associated with loss in GEnC glycocalyx and an increase in albuminuria, suggesting that MMP could be the underlying mechanism in SDC4 ectodomain shedding. It is likely that MMPs have other targets, and that SDC4 loss is one of them. Indeed, MMPs mediate degradation of other proteoglycans,[62] SDC1,[63] tight junction protein ZO-1[64] and the antioxidant enzyme superoxide dismutase.[63] MMPs may also degrade collagens but we did not find any evidence of this in our model of early DKD. Published findings supports that MMPs mediate degradation of endothelial glycocalyx[65-68] and is consistent with published work highlighting MMP2 and 9 cleavage sites on the SDC4 ectodomain.[69]

To determine whether endothelial glycocalyx could be protected or restored in DKD, a pharmacological approach was adopted, and MMPI, a highly selective inhibitor for MMP2 and 9[70] was given therapeutically after the onset of albuminuria. MMPI had no effect on blood glucose, body weight but significantly attenuated the increase in albuminuria. Our glomerular permeability assay confirmed that MMPI reduced the increase in albuminuria by decreasing glomerular albumin permeability in DKD, highlighting the usefulness of our novel assay in detecting benefits of treatments in terms of glomerular permeability. A study carried out in MMP9 deficient mice has shown significant attenuation of albuminuria and hyperfiltration in diabetic nephropathy but without determining its effects on the glycocalyx.[33] We have shown that MMPI treatment protected endothelial glycocalyx by

significantly increasing glycocalyx depth and coverage. The inhibitor had no effect on glomerular ultrastructure including GBM thickness, podocyte foot process and slit diaphragm width. This was as expected given that we did not observe changes in these parameters in our model of early DKD. This data is consistent with our previously published work that treatment with vascular endothelial growth factor A_{165b} and angiopoietin-1 reversed damage to the glomerular endothelial glycocalyx and normalised glomerular permeability in early DKD.[24, 27] Moreover, VEGFC also protected against raised glomerular permeability and ameliorated glycocalyx disruption in diabetic glomeruli.[41]

Blockade of MMP2 and 9 attenuated diabetes-induced changes in glomerular endothelial glycocalyx SDC4, glomerular SDC4 at the mRNA and protein levels, suggesting a reduction in glomerular endothelial SDC4 shedding. We previously observed similar effects in human GEnC, where MMP inhibition attenuated SDC4 mRNA synthesis and SDC4 shedding and, resulting in a reduction in albumin permeability.[16] MMPI attenuated diabetes-induced SDC4 shedding in the plasma but not urine. Our data shows that MMPI has reached the podocytes as it restored the podocyte glycocalyx loss observed in diabetes. So, this suggests that there are potentially different mechanisms contributing to SDC4 shedding in the plasma and urine; the latter being resistant to MMP2 and 9 inhibitor, perhaps other proteases might be responsible for SDC4 shedding in the urine. Future work will determine the relative importance of MMP2 or 9 and their potential cellular sources. We have previously shown in vitro that MMPs produced by GEnC are sufficient to cause SDC4 shedding[16] but circulating immune cells also produce MMPs[71, 72] which may be equally or more important in diabetes in vivo. There a number of upstream signalling pathways (MAP Kinases,[73, 74] NFκB and PKC[65] that have been implicated in MMP activation but there is little context-specific information and further work in this area may identify further targets for therapeutic intervention. For example, we have previously shown that TNFα activates MMPs and TNF inhibitor used in

clinical practice (Etanercept) attenuates glycocalyx loss in an experimental endotoxin model.[75]

Disruption of the endothelial glycocalyx is known to increase albumin excretion *in vivo*[23] and *in vitro*.[16, 20] Endothelial glycocalyx protection or restoration is therefore an attractive therapeutic target not least because the endothelial glycocalyx damage occurs early in DKD when microalbuminuria is present but glomerular ultrastructure is otherwise unaffected, as we show here. Treatment at this stage may prevent down-stream consequence of developing albuminuria. We have demonstrated that MMP2 and 9-mediated SDC4 shedding is the underlying mechanism of endothelial glycocalyx damage in DKD and that this pathway is potentially amenable to therapeutic intervention.

Methods

Animal welfare

All animal experiments were approved by the UK Home Office. Male DBA/2J, 6-week-old (20–25 g) mice, purchased from Charles River UK Limited, Kent, England, were maintained in an environment with controlled temperature (21–24°C) and lighting (12:12h light–dark cycle). Standard laboratory chow and drinking water were provided ad libitum. A period of 1-2 weeks was allowed for animals to acclimatise before any experiments.

Type 1 diabetes model

For induction of diabetes, mice were fasted for 4-6 hours before using the low-dose Diabetic Complications Consortium (DiaComp) protocol.[42] Briefly, streptozotocin (STZ) was given intraperitoneally at 50mg/kg for 5 consecutive days and the mice were culled at 8 or 9 weeks post STZ injection. Glycaemia, by tail-tip blood droplet analysis using a glucometer (ACCU-CHEK Aviva, Roche, Switzerland) and body weight were monitored weekly after STZ. STZ-

injected mice with glycaemia $\geq$ 15mM were considered diabetic and included in the study. The mice were placed in metabolic cages for up to 4 hours to collect urine weekly. Urinary albumin was quantified with a mouse albumin ELISA (Bethyl Laboratories, Inc. Montgomery, TX), and creatinine was measured using an enzymatic spectrophotometric assay (Konelab T-Series 981845; Thermo Fisher Scientific, Vantaa, Finland). Urinary albumin-to-creatinine ratio (uACR) was calculated as previously.[27] At 6 weeks after STZ administration, some mice were given daily intraperitoneal injections of a potent and highly selective MMP2/9 inhibitor (MMPI) biphenylylsulfonylamino-3-phenylpropionic acid[40, 70, 76, 77] (444241, Merck, Middlesex, UK) at 5mg/kg or vehicle (0.05% DMSO in PBS) for 21 days and the mice were culled at 9 weeks. MMPI binds to the zinc ion at the active site of MMP2 and 9, thereby blocking their activities.[78]

For more details on MMPI and tissue collection in Type 1 diabetes model, please see supplementary methods.

Glomerular albumin permeability (Ps'alb) assay

The glomerular Ps'alb assay was carried out as previously.[24] Briefly, Ringer-perfused kidney was sieved in 4% BSA in Ringer solution. Isolated glomeruli were incubated in 36.5µg/ml Octadecyl rhodamine B chloride (R18, O246, ThermoFisher Scientific) for 15 minutes, then washed in 4% Ringer BSA to remove unbound R18 followed by 15 minutes incubation in 30µg/ml AlexaFluor 488-BSA (A13100, ThermoFisher Scientific). An individual glomerulus was trapped on a custom-made petri-dish and the perfusate was switched from 30µg/ml labelled 488-BSA to 30µg/ml unlabelled BSA. A Nikon TIE inverted confocal microscope was used to capture the fluorescence intensity. The rate of decline in fluorescence intensity within the loop of the capillaries for the first minute was used to calculate Ps'alb as previously.[24]

Please see supplementary methods for Electron microscopy, Fluorescence Activated Cell Sorting (FACS), RNA extraction, Real-time PCR and TaqMan qPCR array.

Protein extraction

Isolated glomeruli were homogenised in PBS. Three freeze-thaw cycles were performed to break the cell membranes and the homogenates were centrifuged for 5 minutes at 5000g, at 2-8°C. The supernatant was removed and either assayed immediately or stored at -80°C.

SDC4 ELISA

The concentrations of SDC4 (ectodomain) in mouse glomerular lysate, plasma and urine were quantified using a sandwich enzyme immunoassay (mouse SDC4 ELISA kit, CSB-EL020891MO, Cusabio, Houston, USA) according to the manufacturer's instructions. The concentration of SDC4 was normalized to total protein content as applicable. The fold change of diabetic with MMPI relative to diabetic vehicle was calculated to enable pooling of results from different experiments.

MMP2 and 9 activity assays

MMP2 and 9 Biotrak Activity Assays (GE Healthcare Life Sciences, Buckinghamshire, UK) provide precise quantitation of active MMP2 and 9 in plasma, urine and tissue homogenates. The assays were carried out according to the manufacturer's instructions. The concentration of active MMP2 and 9 was normalized to total protein or creatinine concentration as applicable.

Lectin staining

5 μm paraffin-embedded kidney sections were dewaxed in histoclear followed by rehydration in graded ethanol and a wash is PBS. The sections were incubated in blocking buffer [1% BSA in PBS containing 0.5% Tween (PBX)] for 30 min, followed by endogenous biotin

blocking using a streptavidin/biotin blocking kit (SP-2002, Vector Laboratories). After 2 washes, the sections were incubated with biotinylated MOA (2mg/ml) 1:100, pH 6.8 overnight at 4°C. Buffer only was used as a negative control. After 4 washes, the sections were incubated with streptavidin AF488 (S32354, ThermoFisher Scientific, 1:500), pH 6.8, for 1 hour at room temperature. The nuclei were counterstained with DAPI (Invitrogen; Life Technologies) and the cell membrane labelled with R18 (O246, ThermoFisher Scientific, at 1:1000 dilution), incubating for 10 min. After a 2 min wash in PBS, the coverslips were mounted in Vectashield mounting medium (Vector Laboratories) and examined using either an AF600 LX wide-field fluorescence microscope (Leica Microsystems, Milton Keynes, UK) or a Leica SP5-II confocal laser scanning microscope attached to a Leica DMI 6000 inverted epifluorescence microscope.

Endothelial glycocalyx depth: Peak to Peak analysis

The peak to peak assessment was carried out as.[39, 40] A line (white arrow Fig1Ei) was drawn from the inside to the outside of the capillary loop crossing the glycocalyx first followed by the R18 endothelial membrane. The line is drawn perpendicular to the endothelial glycocalyx and the cell membrane label to get the maximum consistent depth of the glycocalyx. Fluorescence intensity profiles were then generated for both the SDC4 or MOA component of the endothelial glycocalyx and endothelial cell label. The distance between the peak signals from the SDC4/MOA-488 and the R18 labels (peak to peak: P-P) is an index of glycocalyx thickness. P-P was determined from an average of 3 lines in a loop, 3 loops in a glomerulus, 3 glomeruli in a mouse and n=5 mice in each group.

Statistical analysis

Data are expressed as the mean ± SEM. Fold change is defined as the ratio between the two groups specified in the text. Normality was assessed using GraphPad Prism 5 Kolmogorov–

Smirnov test. Normally distributed data was compared using t-tests for 2 groups and analysis of variance (ANOVA) for multiple groups. If one-way ANOVA indicated a significant difference, the Bonferroni post hoc test was used to assess differences between groups. Where normality could not be demonstrated, the Mann-Whitney test was used for comparing between 2 groups. A p value of <0.05 was considered to indicate statistical significance.

Disclosure

There is nothing to disclose.

Supplementary Material

Figure S legends

Figure S1. Early diabetic kidney disease (DKD) is associated with reduced podocyte glycocalyx but not change in other podocyte or GBM parameters. Control and diabetic mice were perfusion-fixed for electron microscopy with cacodylate buffer containing glutaraldehyde and Alcian blue. Representative electron micrographs of the glomerular capillary wall are shown at lower and higher magnification (Ai, ii). The measurements were carried out on 3 capillary loops per glomerulus and 2–3 glomeruli were used per mouse. Labels indicate podocyte glycocalyx (pGLX), basement membrane (GBM, 1), podocyte slit diaphragm width (2) and podocyte foot process width (3) (scale bar =200nm). Quantification of (A, Bi) pGLX depth (control 23.70 ± 2.341 n=5 mice, diabetes 15.06 ± 1.713 n=5 mice, *p=0.0176) and (A, Bii) percentage podocyte with GLX coverage (control 97.78 ± 2.222 n=5 mice, diabetes 79.28 ± 10.57 n=5 mice, non significant (ns)); (A, C) GBM thickness (control 134.2 ± 3.047 n=5, diabetes 138.2 ± 10.89 n=5 mice, ns). (A, D) podocyte slit diaphragm width (control 40.48 ± 1.914 n=5 mice, diabetes 39.79 ± 3.243 n=5 mice, ns); (A. E) podocyte foot process width (control 251.8 ± 17.07 n=5 mice, diabetes 264.9 ± 20.16 n=5 mice, ns). (F, G) Picro Sirius red staining was carried out on control and diabetic kidney sections and representative immunohistochemistry images demonstrate no change in collagen deposition in diabetic glomeruli when compared to control (a minimum of 3 glomeruli were analysed per mouse, control 836500 ± 175700 n=5 mice, diabetes 1060000 ± 339200 n=5(ns)). Each dot or square on the graph represents a mouse. Data is expressed as the mean $\pm$ SEM and unpaired *t* test at week 9 post STZ was used for statistical analysis.

Table S1. List of glycocalyx related genes represented on custom-designed TaqMan qPCR array

Table S2. Expression Suite software and $2^{-\Delta\Delta CT}$ method followed by *t* test were used to analyse the array data and both methods showed a significant increase in SDC1, 3, 4 and MMP14 mRNA expression amongst other significantly modulated gene expression.

Table S3. List of primer probes used in this study

Figure S2. Isolation of mouse glomerular endothelial cells. Mouse glomeruli were isolated by sieving and were digested with collagenase. The single cells obtained were immunolabelled with anti-CD31 antibody. The cells were also stained with propidium iodide to exclude the dead ones. Propidium iodide negative and CD31 positive cells (within the gate) were sorted by a flow cytometry cell sorter to produce pure population of glomerular endothelial cells. The mRNA expression of VEGFR2 (specific for endothelial cells), nephrin (specific for podocyte) and PDGFR2 (specific for mesangial cells), relative to GAPDH was determined. The representative graph shows glomerular endothelial cells had high expression of VEGFR2 but were negative for nephrin and PDGFR2 confirming no or minimal contamination with either podocytes or mesangial cells, n=1 mouse.

Figure S3. Mice were injected intravenously (iv) with 0.05 mg/mouse SDC4 antibody (100μl). After 18 min of incubation, cardiac perfusion with Ringer was performed to flush out unbound antibody. Kidney was snap frozen for immufluorescence staining. (A) Frozen kidney sections were incubated with secondary antibody to SDC4 (Alexa 488, green) and DAPI (blue). Representative images show that the SDC4 antibody localised predominantly to the glomeruli in the SDC4 injected mice and no SDC4 staining can be seen in the PBS injected mice.(B) Frozen kidney sections from SDC4 antibody (red and green) injected mice

were immunostained with CD31 (endothelial, green), podocin (podocytes, red) and DAPI (blue). Representative confocal images show SDC4 colocalises predominantly with endothelial and not podocyte markers.

Table S4 shows the absolute values of albumin, creatinine and albumin creatinine ratio from 3 independent experiments carried out on diabetic (Dia) + MMPI or vehicle (Veh) mice.

Figure S4. Blockade of MMP2 and 9 restored diabetes-induced podocyte glycocalyx loss without affecting other podocyte parameters. Diabetic (Dia) ± MMPI or vehicle (Veh)-treated mice were perfusion-fixed for electron microscopy with cacodylate buffer containing glutaraldehyde and Alcian blue. Representative electron micrographs of the glomerular capillary wall are shown at lower and higher magnification (Ai, ii). The measurements were carried out on 3 capillary loops per glomerulus and 2–3 glomeruli were used per mouse. Labels indicate podocyte glycocalyx (pGLX), basement membrane (GBM, 1), podocyte slit diaphragm width (2) and podocyte foot process width (3) (scale bar =100nm). Quantification of (A, Bi) pGLX depth (Dia Veh 14.88 ± 1.121 n=5 mice, Dia MMPI 25.16 ± 2.777 n=6 mice, *p=0.0112) and (A, Bii) percentage podocyte with GLX coverage (Dia Veh 90.60 ± 8.402 n=5 mice, Dia MMPI 97.30 ± 1.746 n=6 mice, non significant (ns)); (A, C) GBM thickness (Dia Veh 154.1 ± 9.837 n=5 mice, Dia MMPI 149.3 ± 7.904 n=6 mice, ns); (A, D) podocyte slit diaphragm width (Dia Veh 40.12 ± 4.965 n=5 mice, Dia MMPI 35.42 ± 1.155 n=6 mice, ns); (A. E) podocyte foot process width (Dia Veh 302.5 ± 26.76 n=5 mice, Dia MMPI 244.3 ± 13.21 n=6 mice, ns). Each dot or square on the graph represents a mouse. Data is expressed as the mean ± SEM and unpaired *t* test at week 9 post STZ was used for statistical analysis.

Supplementary information is available at Kidney International's website

References

1. Dziembowska M, Pretto DI, Janusz A*, et al.* High MMP-9 activity levels in fragile X syndrome are lowered by minocycline. *Am J Med Genet A* 2013; **161A:** 1897-1903.

2. Chang JJ, Kim-Tenser M, Emanuel BA*, et al.* Minocycline and matrix metalloproteinase inhibition in acute intracerebral hemorrhage: a pilot study. *Eur J Neurol* 2017; **24:** 1384-1391.

3. Gu Y, Walker C, Ryan ME*, et al.* Non-antibacterial tetracycline formulations: clinical applications in dentistry and medicine. *J Oral Microbiol* 2012; **4**.

4. Hex N, Bartlett C, Wright D*, et al.* Estimating the current and future costs of Type 1 and Type 2 diabetes in the UK, including direct health costs and indirect societal and productivity costs. *Diabet Med* 2012; **29:** 855-862.

5. Satchell SC. The glomerular endothelium emerges as a key player in diabetic nephropathy. *Kidney international* 2012; **82:** 949-951.

6. Salmon AH, Satchell SC. Endothelial glycocalyx dysfunction in disease: albuminuria and increased microvascular permeability. *The Journal of pathology* 2012; **226:** 562-574.

7. Satchell S. The role of the glomerular endothelium in albumin handling. *Nat Rev Nephrol* 2013; **9:** 717-725.

8. Reitsma S, Slaaf DW, Vink H*, et al.* The endothelial glycocalyx: composition, functions, and visualization. *Pflugers Arch* 2007; **454:** 345-359.

9. Pyke C, Kristensen P, Ostergaard PB*, et al.* Proteoglycan expression in the normal rat kidney. *Nephron* 1997; **77:** 461-470.

10. Chen S, Wassenhove-McCarthy D, Yamaguchi Y*, et al.* Podocytes require the engagement of cell surface heparan sulfate proteoglycans for adhesion to extracellular matrices. *Kidney international* 2010; **78:** 1088-1099.

11. Adembri C, Sgambati E, Vitali L*, et al.* Sepsis induces albuminuria and alterations in the glomerular filtration barrier: a morphofunctional study in the rat. *Crit Care* 2011; **15:** R277.

12. Rops AL, Gotte M, Baselmans MH*, et al.* Syndecan-1 deficiency aggravates anti-glomerular basement membrane nephritis. *Kidney international* 2007; **72:** 1204-1215.

13. Manon-Jensen T, Itoh Y, Couchman JR. Proteoglycans in health and disease: the multiple roles of syndecan shedding. *The FEBS journal* 2010; **277:** 3876-3889.

14. Multhaupt HA, Yoneda A, Whiteford JR*, et al.* Syndecan signaling: when, where and why? *J Physiol Pharmacol* 2009; **60 Suppl 4:** 31-38.

15. Couchman JR. Transmembrane signaling proteoglycans. *Annu Rev Cell Dev Biol* 2010; **26:** 89-114.

16. Ramnath R, Foster RR, Qiu Y*, et al.* Matrix metalloproteinase 9-mediated shedding of syndecan 4 in response to tumor necrosis factor alpha: a contributor to endothelial cell glycocalyx dysfunction. *FASEB J* 2014; **28:** 4686-4699.

17. Weinbaum S, Tarbell JM, Damiano ER. The structure and function of the endothelial glycocalyx layer. *Annu Rev Biomed Eng* 2007; **9:** 121-167.

18. Singh A, Friden V, Dasgupta I*, et al.* High glucose causes dysfunction of the human glomerular endothelial glycocalyx. *Am J Physiol Renal Physiol* 2011; **300:** F40-48.

19. Singh A, Ramnath RD, Foster RR*, et al.* Reactive oxygen species modulate the barrier function of the human glomerular endothelial glycocalyx. *PLoS One* 2013; **8:** e55852.

20. Singh A, Satchell SC, Neal CR*, et al.* Glomerular endothelial glycocalyx constitutes a barrier to protein permeability. *J Am Soc Nephrol* 2007; **18:** 2885-2893.

21. Jeansson M, Haraldsson B. Morphological and functional evidence for an important role of the endothelial cell glycocalyx in the glomerular barrier. *Am J Physiol Renal Physiol* 2006; **290:** F111-116.

22. Salmon AH, Ferguson JK, Burford JL*, et al.* Loss of the endothelial glycocalyx links albuminuria and vascular dysfunction. *J Am Soc Nephrol* 2012; **23:** 1339-1350.

23. Jeansson M, Haraldsson B. Glomerular size and charge selectivity in the mouse after exposure to glucosaminoglycan-degrading enzymes. *J Am Soc Nephrol* 2003; **14:** 1756-1765.

24. Desideri S, Onions KL, Qiu Y*, et al.* A novel assay provides sensitive measurement of physiologically relevant changes in albumin permeability in isolated human and rodent glomeruli. *Kidney international* 2018.

25. Satoh M, Kobayashi S, Kuwabara A*, et al.* In vivo visualization of glomerular microcirculation and hyperfiltration in streptozotocin-induced diabetic rats. *Microcirculation* 2010; **17:** 103-112.

26. Jeansson M, Granqvist AB, Nystrom JS*, et al.* Functional and molecular alterations of the glomerular barrier in long-term diabetes in mice. *Diabetologia* 2006; **49:** 2200-2209.

27.   Oltean S, Qiu Y, Ferguson JK*, et al.* Vascular Endothelial Growth Factor-A165b Is Protective and Restores Endothelial Glycocalyx in Diabetic Nephropathy. *J Am Soc Nephrol* 2015; **26:** 1889-1904.

28.   Nieuwdorp M, Mooij HL, Kroon J*, et al.* Endothelial glycocalyx damage coincides with microalbuminuria in type 1 diabetes. *Diabetes* 2006; **55:** 1127-1132.

29.   Broekhuizen LN, Lemkes BA, Mooij HL*, et al.* Effect of sulodexide on endothelial glycocalyx and vascular permeability in patients with type 2 diabetes mellitus. *Diabetologia* 2010; **53:** 2646-2655.

30.   Satchell SC, Tooke JE. What is the mechanism of microalbuminuria in diabetes: a role for the glomerular endothelium? *Diabetologia* 2008; **51:** 714-725.

31.   Lauhio A, Sorsa T, Srinivas R*, et al.* Urinary matrix metalloproteinase -8, -9, -14 and their regulators (TRY-1, TRY-2, TATI) in patients with diabetic nephropathy. *Annals of medicine* 2008; **40:** 312-320.

32.   Romanic AM, Burns-Kurtis CL, Ao Z*, et al.* Upregulated expression of human membrane type-5 matrix metalloproteinase in kidneys from diabetic patients. *Am J Physiol Renal Physiol* 2001; **281:** F309-317.

33.   Qing-Hua G, Ju-Ming L, Chang-Yu P*, et al.* The kidney expression of matrix metalloproteinase-9 in the diabetic nephropathy of Kkay mice. *J Diabetes Complications* 2008; **22:** 408-412.

34.   Derosa G, Avanzini MA, Geroldi D*, et al.* Matrix metalloproteinase 2 may be a marker of microangiopathy in children and adolescents with type 1 diabetes mellitus. *Diabetes research and clinical practice* 2005; **70:** 119-125.

35.   Chung AW, Hsiang YN, Matzke LA*, et al.* Reduced expression of vascular endothelial growth factor paralleled with the increased angiostatin expression resulting from the upregulated activities of matrix metalloproteinase-2 and -9 in human type 2 diabetic arterial vasculature. *Circulation research* 2006; **99:** 140-148.

36.   Thrailkill KM, Bunn RC, Moreau CS*, et al.* Matrix metalloproteinase-2 dysregulation in type 1 diabetes. *Diabetes care* 2007; **30:** 2321-2326.

37.   Diamant M, Hanemaaijer R, Verheijen JH*, et al.* Elevated matrix metalloproteinase-2 and -9 in urine, but not in serum, are markers of type 1 diabetic nephropathy. *Diabet Med* 2001; **18:** 423-424.

38.   Li SY, Huang PH, Yang AH*, et al.* Matrix metalloproteinase-9 deficiency attenuates diabetic nephropathy by modulation of podocyte functions and dedifferentiation. *Kidney international* 2014; **86:** 358-369.

39.   Betteridge KB, Arkill KP, Neal CR*, et al.* Sialic acids regulate microvessel permeability, revealed by novel in vivo studies of endothelial glycocalyx structure and function. *J Physiol* 2017; **595:** 5015-5035.

40.   Butler MJ, Ramnath R, Kadoya H*, et al.* Aldosterone induces albuminuria via matrix metalloproteinase-dependent damage of the endothelial glycocalyx. *Kidney international* 2019; **95:** 94-107.

41.   Onions KL, Gamez M, Buckner NR*, et al.* VEGFC Reduces Glomerular Albumin Permeability and Protects Against Alterations in VEGF Receptor Expression in Diabetic Nephropathy. *Diabetes* 2019; **68:** 172-187.

42.   Breyer MD, Bottinger E, Brosius FC, 3rd*, et al.* Mouse models of diabetic nephropathy. *J Am Soc Nephrol* 2005; **16:** 27-45.

43.   Qi Z, Fujita H, Jin J*, et al.* Characterization of susceptibility of inbred mouse strains to diabetic nephropathy. *Diabetes* 2005; **54:** 2628-2637.

44.   Daehn I, Casalena G, Zhang T*, et al.* Endothelial mitochondrial oxidative stress determines podocyte depletion in segmental glomerulosclerosis. *J Clin Invest* 2014; **124:** 1608-1621.

45.   Sun YB, Qu X, Zhang X*, et al.* Glomerular endothelial cell injury and damage precedes that of podocytes in adriamycin-induced nephropathy. *PLoS One* 2013; **8:** e55027.

46.   Kanetsuna Y, Takahashi K, Nagata M*, et al.* Deficiency of endothelial nitric-oxide synthase confers susceptibility to diabetic nephropathy in nephropathy-resistant inbred mice. *Am J Pathol* 2007; **170:** 1473-1484.

47.   Rabelink TJ, de Zeeuw D. The glycocalyx--linking albuminuria with renal and cardiovascular disease. *Nat Rev Nephrol* 2015; **11:** 667-676.

48.   Dane MJ, van den Berg BM, Avramut MC*, et al.* Glomerular endothelial surface layer acts as a barrier against albumin filtration. *Am J Pathol* 2013; **182:** 1532-1540.

49.   Zoja C, Benigni A, Remuzzi G. Cellular responses to protein overload: key event in renal disease progression. *Curr Opin Nephrol Hypertens* 2004; **13:** 31-37.

50.   Haddad G, Zhu LF, Rayner DC*, et al.* Experimental glomerular endothelial injury in vivo. *PLoS One* 2013; **8:** e78244.

51.   Warner RL, Winter HC, Speyer CL*, et al.* Marasmius oreades lectin induces renal thrombotic microangiopathic lesions. *Exp Mol Pathol* 2004; **77:** 77-84.

52.   Ebong EE, Macaluso FP, Spray DC*, et al.* Imaging the endothelial glycocalyx in vitro by rapid freezing/freeze substitution transmission electron microscopy. *Arterioscler Thromb Vasc Biol* 2011; **31:** 1908-1915.

53.   Fan Q, Shike T, Shigihara T*, et al.* Gene expression profile in diabetic KK/Ta mice. *Kidney international* 2003; **64:** 1978-1985.

54.   Svennevig K, Kolset SO, Bangstad HJ. Increased syndecan-1 in serum is related to early nephropathy in type 1 diabetes mellitus patients. *Diabetologia* 2006; **49:** 2214-2216.

55.   Boels MG, Avramut MC, Koudijs A*, et al.* Atrasentan Reduces Albuminuria by Restoring the Glomerular Endothelial Glycocalyx Barrier in Diabetic Nephropathy. *Diabetes* 2016; **65:** 2429-2439.

56.   Dogne S, Flamion B, Caron N. Endothelial Glycocalyx as a Shield Against Diabetic Vascular Complications: Involvement of Hyaluronan and Hyaluronidases. *Arterioscler Thromb Vasc Biol* 2018; **38:** 1427-1439.

57.   Peeters SA, Engelen L, Buijs J*, et al.* Plasma matrix metalloproteinases are associated with incident cardiovascular disease and all-cause mortality in patients with type 1 diabetes: a 12-year follow-up study. *Cardiovasc Diabetol* 2017; **16:** 55.

58.   van der Zijl NJ, Hanemaaijer R, Tushuizen ME*, et al.* Urinary matrix metalloproteinase-8 and -9 activities in type 2 diabetic subjects: A marker of incipient diabetic nephropathy? *Clin Biochem* 2010; **43:** 635-639.

59.   McKittrick IB, Bogaert Y, Nadeau K*, et al.* Urinary matrix metalloproteinase activities: biomarkers for plaque angiogenesis and nephropathy in diabetes. *Am J Physiol Renal Physiol* 2011; **301:** F1326-1333.

60.   Ebihara I, Nakamura T, Shimada N*, et al.* Increased plasma metalloproteinase-9 concentrations precede development of microalbuminuria in non-insulin-dependent diabetes mellitus. *Am J Kidney Dis* 1998; **32:** 544-550.

61.   Hernandez-Perez M, El-hajahmad M, Massaro J*, et al.* Expression of gelatinases (MMP-2, MMP-9) and gelatinase activator (MMP-14) in actinic keratosis and in in situ and invasive squamous cell carcinoma. *Am J Dermatopathol* 2012; **34:** 723-728.

62.   Lipowsky HH. Protease Activity and the Role of the Endothelial Glycocalyx in Inflammation. *Drug Discov Today Dis Models* 2011; **8:** 57-62.

63.   Ali MM, Mahmoud AM, Le Master E*, et al.* Role of matrix metalloproteinases and histone deacetylase in oxidative stress-induced degradation of the endothelial glycocalyx. *Am J Physiol Heart Circ Physiol* 2019; **316:** H647-H663.

64. Cui N, Wang H, Long Y*, et al.* Dexamethasone Suppressed LPS-Induced Matrix Metalloproteinase and Its Effect on Endothelial Glycocalyx Shedding. *Mediators Inflamm* 2015; **2015:** 912726.

65. Fitzgerald ML, Wang Z, Park PW*, et al.* Shedding of syndecan-1 and -4 ectodomains is regulated by multiple signaling pathways and mediated by a TIMP-3-sensitive metalloproteinase. *J Cell Biol* 2000; **148:** 811-824.

66. Mulivor AW, Lipowsky HH. Inhibition of glycan shedding and leukocyte-endothelial adhesion in postcapillary venules by suppression of matrixmetalloprotease activity with doxycycline. *Microcirculation* 2009; **16:** 657-666.

67. Cooper S, Emmott A, McDonald KK*, et al.* Increased MMP activity in curved geometries disrupts the endothelial cell glycocalyx creating a proinflammatory environment. *PLoS One* 2018; **13:** e0202526.

68. Cooper S, McDonald K, Burkat D*, et al.* Stenosis Hemodynamics Disrupt the Endothelial Cell Glycocalyx by MMP Activity Creating a Proinflammatory Environment. *Ann Biomed Eng* 2017; **45:** 2234-2243.

69. Manon-Jensen T, Multhaupt HA, Couchman JR. Mapping of matrix metalloproteinase cleavage sites on syndecan-1 and syndecan-4 ectodomains. *The FEBS journal* 2013; **280:** 2320-2331.

70. Tamura Y, Watanabe F, Nakatani T*, et al.* Highly selective and orally active inhibitors of type IV collagenase (MMP-9 and MMP-2): N-sulfonylamino acid derivatives. *J Med Chem* 1998; **41:** 640-649.

71. Seifert R, Kuhlmann MT, Eligehausen S*, et al.* Molecular imaging of MMP activity discriminates unstable from stable plaque phenotypes in shear-stress induced murine atherosclerosis. *PLoS One* 2018; **13:** e0204305.

72. Reel B, Sala-Newby GB, Huang WC*, et al.* Diverse patterns of cyclooxygenase-independent metalloproteinase gene regulation in human monocytes. *Br J Pharmacol* 2011; **163:** 1679-1690.

73. Alexander JP, Acott TS. Involvement of the Erk-MAP kinase pathway in TNFalpha regulation of trabecular matrix metalloproteinases and TIMPs. *Invest Ophthalmol Vis Sci* 2003; **44:** 164-169.

74. Sondergaard BC, Schultz N, Madsen SH*, et al.* MAPKs are essential upstream signaling pathways in proteolytic cartilage degradation--divergence in pathways leading to aggrecanase and MMP-mediated articular cartilage degradation. *Osteoarthritis Cartilage* 2010; **18:** 279-288.

75.   Nieuwdorp M, Meuwese MC, Mooij HL*, et al.* Tumor necrosis factor-alpha inhibition protects against endotoxin-induced endothelial glycocalyx perturbation. *Atherosclerosis* 2009; **202:** 296-303.

76.   Li H, Mittal A, Makonchuk DY*, et al.* Matrix metalloproteinase-9 inhibition ameliorates pathogenesis and improves skeletal muscle regeneration in muscular dystrophy. *Human molecular genetics* 2009; **18:** 2584-2598.

77.   Yamaguchi M, Jadhav V, Obenaus A*, et al.* Matrix metalloproteinase inhibition attenuates brain edema in an in vivo model of surgically-induced brain injury. *Neurosurgery* 2007; **61:** 1067-1075; discussion 1075-1066.

78.   Vandenbroucke RE, Libert C. Is there new hope for therapeutic matrix metalloproteinase inhibition? *Nat Rev Drug Discov* 2014; **13:** 904-927.

Acknowledgements

Figure legends

Figure 1. Glomerular endothelial glycocalyx damage accompanies albuminuria in early diabetic kidney disease (DKD). Streptozotocin (STZ) was given for 5 consecutive days. Two weeks after the first STZ injection, mice became hyperglycemic which persisted until the mice were culled after week 8 post STZ. (Ai) Glycemia at week 2 (control 6.717 ± 0.1278 n=12 mice, diabetes 19.78 ± 1.441 n=12 mice, *** p<0.0001) and week 8 post STZ (control 6.750 ± 0.1517 n=6 mice, diabetes 28.22 ± 1.586 n=6 mice, *** p<0.0001). (Aii) Body weight, not significant (ns) (n=6 mice each group) when compared to baseline (prior to STZ injection) but significantly lower than control mice at week 8 post STZ (control 30.08 ± 0.9420 n=6 mice, diabetes 24.88 ± 0.7641 n=6 mice, ** p=0.0016). (Bi) Urinary albumin creatinine ratio (uACR) was determined post STZ injection. Week 6 (control 43.94 ± 6.073 n=5 mice, diabetes 243.1 ± 77.26 n=5 mice, *p=0.0332), week 7 (control 43.21 ± 5.644 n=12 mice, diabetes 209.4 ± 67.88 n=10 mice, *p=0.0143) and week 8 post STZ (control 42.81 ± 3.352 n=10 mice, diabetes 208.3 ± 67.74 n=10 mice, *p=0.0253). (Bii) Isolated glomeruli from control and diabetic mice were incubated with R18 then Alexa Fluor 488 bovine serum albumin (AF488-BSA), and glomerular albumin permeability (Ps'alb) was measured at week 9 post STZ. Data is presented as control 3.249 ± 0.2063 n=25 glomeruli, diabetes 5.806 ± 0.3553 n=22 glomeruli, *** p<0.0001. The data was also analysed in terms of mouse number at week 9 post STZ (control $3.144 \times 10^{-7} \pm 2.947 \times 10^{-8}$ n=5, diabetes $5.857 \times 10^{-7} \pm 2.788 \times 10^{-8}$ n=5 mice, *** p<0.0001. (1C) Representative electron micrographs of the glomerular capillary wall are shown. The measurements were carried out on 3 capillary loops per glomerulus and 2–3 glomeruli were used per mouse. Labels indicate endothelial glycocalyx (eGLX), glomerular basement membrane (GBM) and podocyte glycocalyx (pGLX) (scale bar=200nm). Quantification at week 9 post STZ of (Di) endothelial glycocalyx (eGLX) depth (control 24.21 ± 2.550 n=5 mice, diabetes 12.69 ± 1.755 n=5 mice, * * 0.0059); (Dii)

percentage endothelium with GLX coverage (control 95.19 ± 2.139 n=5 mice, diabetes 63.32 ± 15.35 n=5 mice, (ns) non significant). (1Ei) Control and diabetic sections were stained with Marasmium oreades agglutinin (MOA) lectin and endothelial membrane label R18. Representative image shows glomerular capillaries labelled red (R18) and the luminal endothelial glycocalyx labelled green (MOA). (Eii) Peak to Peak assessment of the glomerular endothelial glycocalyx at week 9 post STZ showed a significant reduction in glycocalyx thickness in diabetes (control 336.0 ± 26.33 n=5 mice, diabetes 219.0 ± 38.82 n=5 mice, * p=0.04). Each dot/triangle/square on the graph represents a mouse. Data is expressed as the mean ± SEM and unpaired *t* test was used for statistical analysis.

Figure 2. Glycocalyx-related gene expression is modified in early diabetic kidney disease (DKD). (A) Glomerular mRNA expression of SDCs and MMPs relative to GAPDH from control mice was determined. *** $p < 0.0005$, one way ANOVA with Bonferroni as a post hoc test at week 8 post STZ, n=6 mice for all the genes except n=4 mice for MMP 14. (B) A custom-designed TaqMan qPCR array was used to identify changes in glycocalyx-related gene expression in DKD. The $2^{-\Delta\Delta CT}$ method of quantification was used to calculate the fold change relative to control, * $p < 0.05$, ** $p < 0.005$, unpaired *t* test (control n=6 mice, diabetes n=4 mice for all the genes except control n=4 mice, diabetes n=4 mice for MMP14 and diabetes n=3 mice for MMP 9). (C) Genes of interest were validated using independent qPCR (control n=6 mice, diabetes n=4 mice), * $p < 0.05$, ** $p < 0.005$, ***$p < 0.0005$, unpaired *t* test at week 8 post STZ. Each dot on the graph represents a mouse.

Figure 3. SDC4 mRNA and protein are altered in early diabetic kidney disease (DKD). Glomerular endothelial cells (GEnC) were sorted by FACS and (A) SDC4 and (B) SDC1 mRNA expression were determined. The $2^{-\Delta\Delta CT}$ method of quantification was used to

calculate the fold change, normalised to GAPDH, at week 8 post STZ, (SDC4: control 1.000 ± 0.2565 n=9 mice, diabetes 2.470 ± 0.6580 n=8 mice, * p<0.05 ; SDC1: control 1.000 ± 0.1112 n=5 mice, diabetes 1.663 ± 0.4289 n=5 mice, non significant (ns)). Control and diabetic kidney sections were labelled with SDC4 (green) and endothelial membrane label R18 (red). (C) Peak to Peak assessment of the glomerular endothelial glycocalyx using SDC4 labelling at week 9 post STZ showed a significant reduction in glycocalyx SDC4 in diabetes (control 182.5 ± 12.04 n=5 mice, diabetes 64.31 ± 6.513 n=5 mice, *** p<0.0001). Isolated glomerular lysates from control and diabetic mice were used to determine (D) SDC4 and (E) SDC1 concentration using SDC4 & 1 ectodomain ELISA. The data was then normalised to total protein content. SDC4 (control 1.327 ± 0.1439 n=6 mice, diabetes 0.8059 ± 0.1218 n=6 mice, * p<0.05; SDC1 (control 9.671 ± 1.742 n=6, diabetes 9.699 ± 1.313 n=6 mice, non significant (ns)) at week 8 post STZ. SDC4 shedding in the (F) plasma and (G) urine was determined in DKD using the SDC4 ectodomain ELISA at week 8 post STZ. For plasma, control 2.631 ± 0.2860 n=6 mice, diabetes 4.801 ± 0.3793 n=6 mice, **p<0.005. Urine SDC4 was normalised to creatinine (control 3.343 ± 0.9410 n=4 mice, diabetes 39.32 ± 13.03 n=4 mice, * p<0.05, Mann Whitney test at week 8 post STZ). Each dot or square on the graph represents a mouse. Data is expressed as the mean ± SEM and unpaired *t* test was used for statistical analysis unless specified.

Figure 4. MMP activity is altered in multiple compartments in early diabetic kidney disease (DKD). Renal cortex lysates from control and diabetic mice were used to determine (A) MMP2 (control 5.462 ± 0.3652, n=4 mice, diabetes 9.797 ± 1.753, n=6 mice) and (D) MMP9 (control 41.34 ± 3.85, n=4 mice, diabetes 73.12 ± 9.85, n=6 mice) activities using MMP2 and 9 biotrak activity assays. The data was then normalised to total protein content at week 8 post STZ, ** p=0.0095, Mann Whitney test, ** p=0.037, unpaired *t* test were carried out

respectively. Systemic circulation of (B) plasma MMP2 (control 2.232 ± 0.2873 n=11 mice, diabetes 3.285 ± 0.3760 n=10 mice *p=0.0365), (C) urine MMP2 (control 0.03142 ± 0.01251 n=6 mice, diabetes 0.1002 ± 0.01577 n=10 mice ** p=0.0091), (E) plasma MMP9 (control 1.053 ± 0.1014 n=6 mice, diabetes 1.920 ± 0.2262 n=6 mice ** p=0.0058) and (F) urine MMP9 (control 0.1264 ± 0.03644 n=5, diabetes 0.3196 ± 0.03456 n=10 mice ** p=0.0080 Mann Whitney test) activities were determined in DKD. Urine MMP2 and MMP9 were normalised to urine creatinine at week 8 post STZ. Each dot or square on the graph represents a mouse. Data is expressed as the mean ± SEM and unpaired t test was used for statistical analysis unless specified.

Figure 5. MMPs mediate disruption of the glomerular endothelial glycocalyx in early diabetic kidney disease (DKD). (A) Schematic overview of the procedure, 5 daily injections of STZ was given at week 0. Six weeks post STZ injection, MMP2/9 inhibitor (MMPI) was given for 21 days and mice were culled at week 9 post STZ injection. MMPI had no significant effect on (B) glycemia (Dia Veh 31.43 ± 0.8017 n=13 mice, Dia MMPI 31.09 ± 0.6403 n=14 mice, non significant (ns)) and (C) body weight (Dia Veh 23.88 ± 1.044 n=13 mice, Dia MMPI 24.83 ± 0.9469 n=14 mice, ns). (D)Treatment with MMPI reduced urine albumin creatinine ratio (uACR) (Dia Veh 1.000 ± 0.2093 n=18 mice, Dia MMPI 0.3925 ± 0.077 n=13 mice * p=0.0172, Mann Whitney test at week 9 post STZ). The fold change of diabetic MMPI relative to diabetic vehicle was calculated to enable pooling of results from different experiments. (E) Isolated glomeruli from diabetic (Dia) + MMPI or vehicle (Veh) mice were incubated with R18 then Alexa Fluor 488 bovine serum albumin (AF488-BSA), and glomerular albumin permeability (Ps'alb) was measured. Data is presented as Dia Veh 6.438 ± 0.4302 n=10 glomeruli, Dia MMPI 3.081 ± 0.4858 n=10 glomeruli, *** P<0.0001. The data was also analysed in terms of mouse number (Dia Veh $6.533 \times 10^{-7} \pm 2.450 \times 10^{-8}$ n

=3, 3.035 X 10^{-7} ± 2.963 X 10^{-8} n=3 mice, *** p=0.0008). (F) Diabetic (Dia) + MMPI or vehicle (Veh) mice were perfusion-fixed for electron microscopy with cacodylate buffer containing glutaraldehyde and Alcian blue. Representative electron micrographs of the glomerular capillary wall are shown. The measurements were carried out on 3 capillary loops per glomerulus and 2–3 glomeruli were used per mouse. Labels indicate endothelial glycocalyx (eGLX), glomerular basement membrane (GBM) and podocyte glycocalyx (pGLX) (scale bar =100nm). Quantification of (Gi) endothelial glycocalyx (eGLX) depth (Dia Veh 20.69 ± 0.5772 n=5 mice, Dia MMPI 32.91 ± 4.186 n=6 mice, * p=0.0276). (Gii) percentage endothelium with GLX coverage (Dia Veh 52.74 ± 8.411 n=5 mice, Dia MMPI 92.56 ± 5.383 n=6 mice, ** p=0.0026). Each dot or square on the graph represents a mouse. Data is expressed as the mean ± SEM and unpaired *t* test at week 9 post STZ was used for statistical analysis unless specified.

Figure 6. Blockade of MMP2 and 9 ameliorates diabetes-induced changes in SDC4 and reduces plasma MMP activity. Diabetic (Dia) + MMPI or vehicle (Veh)-treated kidney sections were labelled with SDC4 (green) and endothelial membrane label R18 (red). (A) Peak to Peak assessment of the glomerular endothelial glycocalyx using SDC4 labelling at week 9 post STZ showed a significant restoration in glycocalyx thickness (Dia Veh 109.2 ± 9.003 n=5 mice, Dia MMPI 246.0 ± 22.36 n=5 mice, *** p=0.0005). (B) Isolated glomerular lysate from diabetic (Dia) + MMPI or vehicle (Veh)-treated mice was used to determine SDC4 mRNA expression. The $2^{-\Delta\Delta CT}$ method of quantification was used to calculate the fold change, normalised to GAPDH and relative to Dia Veh, (Dia Veh 1.000 ± 0.089 n=11 mice, Dia MMPI 0.6658 ± 0.04849 n=12 mice, ** p=0.0029). (C). Isolated glomerular lysate from diabetic (Dia) + MMPI or vehicle (Veh)-treated mice were used to determine SDC4 concentration with previously used SDC4 ectodomain ELISA. The data was then normalised

to total protein content, (Dia Veh 0.6426 ± 0.06780 n=5 mice, Dia MMPI 1.150 ± 0.1634 n=7

mice, *p=0.0322). MMPI attenuated SDC4 shedding in the (D) plasma (Dia Veh 1.000 ±

0.1029 n=11 mice, Dia MMPI 0.5449 ± 0.09749 n=9 mice, **p=0.0054),but not in the (E)

urine (Dia Veh 1.000 ± 0.1895 n=13 mice, Dia MMPI 0.8501 ± 0.1290 n=8 mice, non

significant (ns)) in DKD. The fold change of diabetic MMPI relative to diabetic vehicle was

calculated to enable pooling of results from different experiments. (F, G) Plasma MMP2 (Dia

Veh 3.001 ± 0.3977 n=13 mice, Dia MMPI 1.528 ± 0.4924 n=7 mice, *p=0.0366) and 9 (Dia

Veh 1.150 ± 0.07157 n=9 mice, Dia MMPI 0.9266 ± 0.03281 n=6 mice, *p=0.0314)

activities, using MMP2 and 9 biotrak activity assays, were reduced in diabetic (Dia) + MMPI

group when compared to diabetic (Dia) + vehicle (Veh) group. Each dot or square on the

graph represents a mouse. Data is expressed as the mean ± SEM and unpaired *t* test at week 9

post STZ was used for statistical analysis unless specified.

Supplementary Methods

Tissue collection in Type 1 diabetes model

Control, diabetic with or without the MMPI inhibitor/vehicle were culled for tissue collection at 8 or 9 weeks post STZ injection. MMP inhibitor is an N-sulfonyl amino acid derivative modified in the amino acid residue and the sulfonamide moiety. Studies carried out on its enzymatic activity have shown that the sulfonamide derivatives containing biaryl, triple bond, tetrazole, or amide were selective inhibitors of type IV collagenase (MMP-9 and MMP-2) in vitro as well as in vivo.[S1] This highly potent and selective inhibitor blocks MMP2 (IC50 = 310 nM) and 9 (IC50 = 240 nM) without affecting other metalloproteinases. [S1] MMPI is easily absorbed across the gastrointestinal tract. [S2, S3] It has been shown to provide protective effects in several disease states: reduce brain edema and preserves the Blood Brain Barrier in a brain injury model, [S4] ameliorates pathogenesis and improves skeletal muscle regeneration in muscular dystrophy [S2] and attenuates albuminuria in an aldosterone-induced kidney disease model. [S3]

For tissue collection, some mice were anaesthetised with 3.5% isoflurane in 1L/min O_2. A midline laparotomy was performed, and the abdominal aorta was cannulated with PE-10 tubing (Becton Dickinson, 427400, Franklin Lakes, NJ) to flush both kidneys with Ringer solution (NaCl, 132mM; KCl, 4.6mM; MgSO4-7H2O 1.27mM; CaCl2-2H2O 2mM; NaHCO3, 25mM; D(+)glucose, 5.5mM; N-2-hydroxyethylpiperazine-N'-2-ethanesulphonic (HEPES) acid, 3.07mM; HEPES sodium salt, 1.9mM, pH 7.40). One kidney was removed for glomerular sieving as previously [S5] and the other kidney was perfusion-fixed with a solution containing 2.5% glutaraldehyde, 0.1M cacodylate and 1% Alcian blue for transmission electron microscopy to quantifying endothelial glycocalyx depth and coverage. [S6] In other mice, instead of perfusion, blood was collected for plasma isolation and the kidneys used for

glomerular sieving. Some mice were intravenously (iv) injected with 0.05 mg/mouse SDC4 antibody. After 18 min of incubation, cardiac perfusion with Ringer was performed to flush out unbound antibody. Kidney was snap frozen for immunofluorescence staining.

Electron microscopy

Electron micrographs were taken using a Technai 12 electron microscope (FEI, Hillsboro, Oregon) and image analysis was carried out as previously in 3 capillary loops per glomerulus and 2–3 glomeruli per animal. [S5, S6] Briefly, ImageJ software (SciJava software ecosystem, Maryland, USA) was used to overlay a grid onto the electron micrograph. The anatomical distance from the luminal phospholipid at sequential grid intersections to the furthest point of glycocalyx was measured as glycocalyx depth. A glycocalyx depth $\leq$ 10nm was considered uncovered and this was expressed as a percentage of total measurements taken on a grid section. Glycocalyx coverage expressed as a percentage = 100% - glycocalyx uncovered%. GBM thickness, podocyte foot process width and slit diaphragm width were also measured. Observers were blinded to sample identity before analysis.

Fluorescence Activated Cell Sorting (FACS)

Mouse glomeruli were collected from 75µm pore sieves as previously. [S5] The glomeruli were digested with 1mg/ml collagenases (1, V, VI) (Sigma-Aldrich, Dorset, UK) for 1 hour at 37°C in a hybridization oven with constant rotation. After the enzymatic digestion was complete, the digest was passed through a 35µm mesh cell strainer (BD falcon 352235, ThermoFisher Scientific) to give a single cell suspension. After 3 washes, the cell pellet was resuspended in HBSS containing 1mM EDTA, 0.1ul/ml DNAse and 0.3% BSA (Sigma-Aldrich) and immunostained with PE Rat Anti-Mouse CD31 antibody (BD Pharmingen, San Jose, CA) at a 1:50 dilution for 1 hour at 4°C. After 3 washes, the cells were ready for FACS. CD31 positive cells were isolated using a Becton Dickinson Influx Cell Sorter (BD Biosciences, San Jose,

CA). In brief, single viable cells were detected based on laser scatter, trigger pulse width and exclusion of the vital dye Propidium Iodide (PI). Cells were excited with 488nm and 552nm lasers and fluorescence emissions were captured for PE (552nm 582/29nm BP) and PI (552nm 710/50 BP) respectively. Controls included were unstained cells and isotype control (Rat IgG2a, κ Isotype Control, FITC Goat Anti-Rat Igs, BD Pharmingen).

RNA extraction

RNA was extracted from isolated glomeruli using an RNeasy Mini kit (Qiagen, Manchester, UK) according to manufacturer's instructions. Then 2μg of total RNA was converted to cDNA by a high-capacity RNA to cDNA conversion kit (Applied Biosystems, Foster City, CA, USA), according to the manufacturer's instructions.

Real-time PCR

The mRNA expression of relevant genes was quantified according to the manufacturer's instructions for real-time PCR (StepOnePlus Real-Time PCR System; Applied Biosystems) using TaqMan primer probes (Life Technologies, ThermoFisher Scientific) detailed in supplementary Table 3. PCRs were performed in duplicate. The $2^{-\Delta\Delta CT}$ method was used to calculate the fold change, normalized to GAPDH.

TaqMan qPCR array

The custom-designed TaqMan Low Density Array (TLDA, Applied Biosystems) is a 384-well microfluidic card that performs 384 simultaneous real-time PCR. We designed an array which included 53 glycocalyx-related and control genes (Table 2, supplementary material). cDNA (1:5 dilution) and TaqMan gene expression master mix (Applied Biosystems) were used to perform the reaction. In brief, the wells of the TaqMan array contained TaqMan gene expression assays that detected the real-time amplification of the specified targets. Relative levels of gene expression were determined from the fluorescence data generated during PCR

using a ViiA7 Real-Time PCR System (Applied Biosystems). Expression Suite software (ThermoFisher scientific) which utilises the comparative Cτ (ΔΔCτ) method was used to rapidly and accurately quantify relative gene expression across a large number of genes and samples. For the selected genes of interest, the $2^{-\Delta\Delta CT}$ method was also used to calculate fold changes, normalized to GAPDH. Independent *t*-tests with $p < 0.05$ were used as a screening test, and genes that were significantly modulated (and MMP9 in view of previous results) [S7] were selected for further analysis by independent real-time PCR.

Immunofluorescence staining

5 µm cut frozen kidney sections were fixed with 4% paraformaldehyde. The sections were incubated in blocking solution [1% bovine serum albumin (BSA) in PBS containing 0.1% Tween] for 1 hour. Some sections from the SDC4 (Purified Rat Anti-Mouse Syndecan-4, Clone KY/8.2, BD Biosciences) injected mice were incubated with Alexa Fluor™ 488 secondary antibody (Molecular Probes; Life Technologies). Others were incubated with primary antibodies to either CD31 (FITC Rat Anti-Mouse CD31MEC13.3, BD Biosciences at 1:100 dilution) or podocin (P0372, Sigma-Aldrich, at 1:500 dilution) in blocking buffer for 40 min at room temperature. Primary antibody binding was detected by using Alexa Fluor™ 488 and 633 secondary antibodies (Molecular Probes; Life Technologies). After 3 washes, the nuclei were counterstained with 4′,6-diamidino-2-phenylindole dihydrochloride (DAPI; Invitrogen; Life Technologies). For peak to peak analysis, the sections were incubated with an endothelial cell membrane label R18 (O246, ThermoFisher Scientific, at 1:1000 dilution) for 10 min. After a 2 min wash in PBS, the coverslips were mounted in Vectashield mounting medium (Vector Laboratories, Peterborough, UK) and examined using either an AF600 LX wide-field fluorescence microscope (Leica Microsystems, Milton Keynes, UK) or a Leica SP5-II confocal laser scanning microscope attached to a Leica DMI 6000 (Leica Microsystems) inverted epifluorescence microscope.

Picrosirius Red Staining

Picrosirius Red Staining was carried out as. [S8] Mouse paraffin tissue sections were hydrated followed by counterstaining in a 0.1% (w/v) Direct Red 80 powder (SigmaAldrich) in a 1.3% saturated aqueous solution of picric acid (VWR Chemicals) for 90 min at room temperature, then dehydrated and mounted. Images were taken using a bright-field microscope. Images were quantified using Image J. A minimum of 3 glomeruli were analysed per mouse and n=5 mice per group. Images were converted to RGB images and colour deconvolution was performed. Red staining channel was then converted to 8-bit gray scale image and colour inverted. Total of 4 background mean gray value measurements were taken. Tracing tool was used to draw around glomerulus to measure area and integrated density. Corrected Total Cell Fluorescence (CTCF) was then calculated by subtracting the average of background mean gray values multiplied by area of glomerulus from glomerular integrated density. CTCF values for each mouse were then averaged and plotted.

Supplementary references

S1.   Tamura Y, Watanabe F, Nakatani T, *et al.* Highly selective and orally active inhibitors of type IV collagenase (MMP-9 and MMP-2): N-sulfonylamino acid derivatives. *J Med Chem* 1998; **41:** 640-649.

S2.   Li H, Mittal A, Makonchuk DY, *et al.* Matrix metalloproteinase-9 inhibition ameliorates pathogenesis and improves skeletal muscle regeneration in muscular dystrophy. *Human molecular genetics* 2009; **18:** 2584-2598.

S3.   Butler MJ, Ramnath R, Kadoya H, *et al.* Aldosterone induces albuminuria via matrix metalloproteinase-dependent damage of the endothelial glycocalyx. *Kidney international* 2019; **95:** 94-107.

S4.   Yamaguchi M, Jadhav V, Obenaus A, *et al.* Matrix metalloproteinase inhibition attenuates brain edema in an in vivo model of surgically-induced brain injury. *Neurosurgery* 2007; **61:** 1067-1075; discussion 1075-1066.

S5.   Desideri S, Onions KL, Qiu Y, *et al.* A novel assay provides sensitive measurement of physiologically relevant changes in albumin permeability in isolated human and rodent glomeruli. *Kidney international* 2018.

S6.   Oltean S, Qiu Y, Ferguson JK, *et al.* Vascular Endothelial Growth Factor-A165b Is Protective and Restores Endothelial Glycocalyx in Diabetic Nephropathy. *J Am Soc Nephrol* 2015; **26:** 1889-1904.

S7.   Ramnath R, Foster RR, Qiu Y, *et al.* Matrix metalloproteinase 9-mediated shedding of syndecan 4 in response to tumor necrosis factor alpha: a contributor to endothelial cell glycocalyx dysfunction. *FASEB J* 2014; **28:** 4686-4699.

S8.   Onions KL, Gamez M, Buckner NR, *et al.* VEGFC Reduces Glomerular Albumin Permeability and Protects Against Alterations in VEGF Receptor Expression in Diabetic Nephropathy. *Diabetes* 2019; **68:** 172-187.

Figure 1

Figure 2

Figure 3

Figure 4

Figure 5

A

STZ

MMPI

Hyperglycemia

Wk0   Wk1   Wk6   Wk9

B

Blood glucose (mM)

△ Dia Veh
○ Dia MMPI

Time (weeks post stz)

C

Body weight (g)

△ Dia Veh
○ Dia MMPI

Time (weeks post stz)

D

uACR relative to Dia Veh (mg/mmol)

*

Dia Veh   Dia MMPI

E

Ps' alb (cm/s x 10^{-7})

***

Dia Veh   Dia MMPI

F

Diabetes Vehicle

eGLX   GBM   pGLX   100 nm

Diabetes MMPI

eGLX   GBM   pGLX   100 nm

Gi

Glycocalyx depth (nm)

*

Dia Veh   Dia MMPI

Gii

Glycocalyx coverage (%)

**

Dia Veh   Dia MMPI
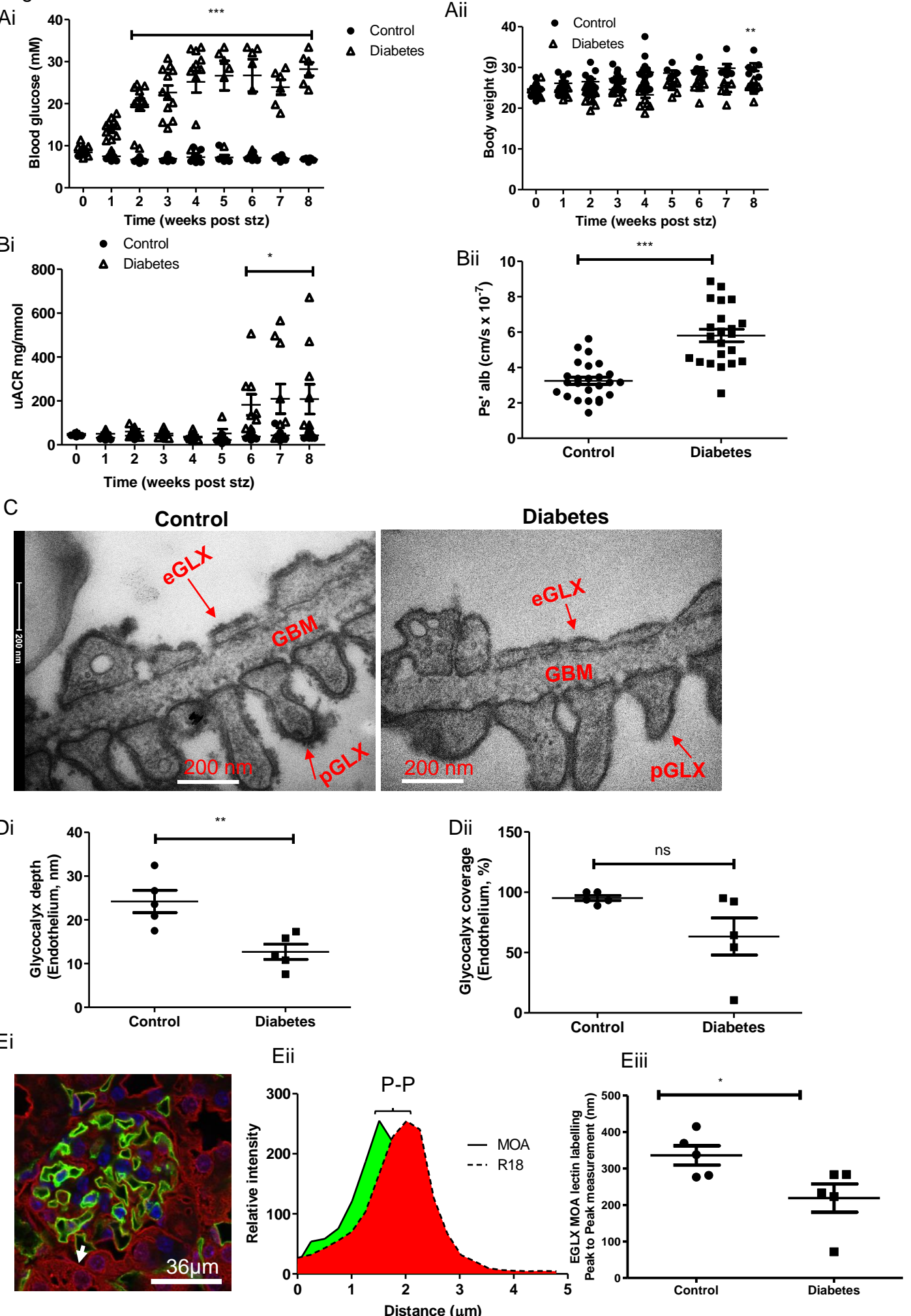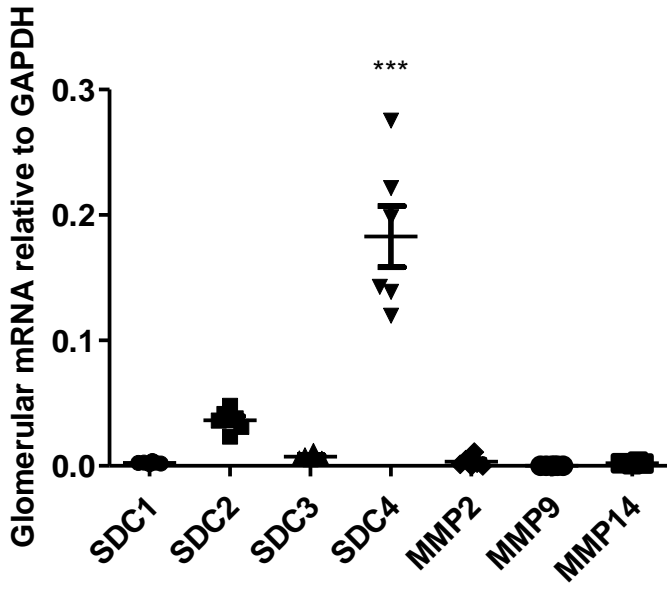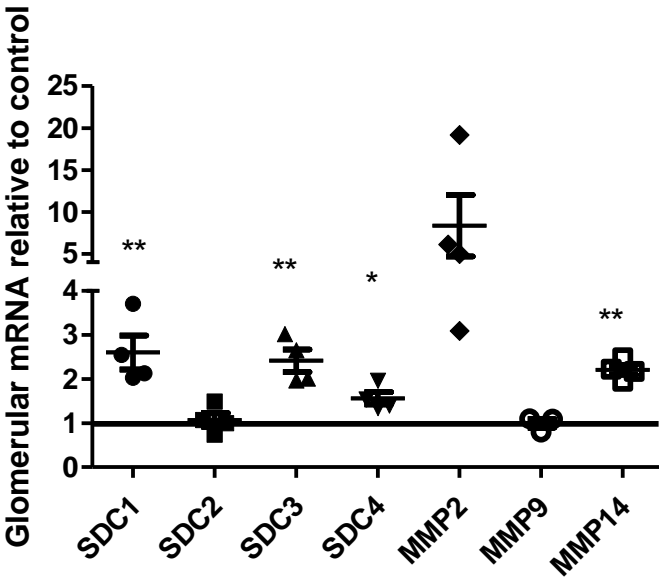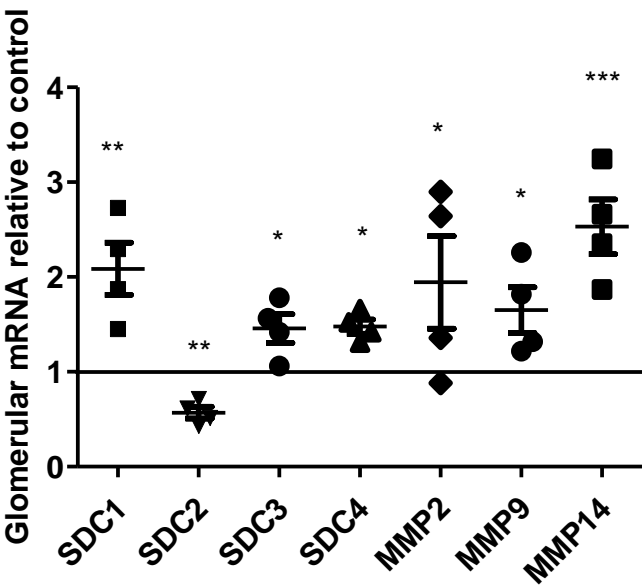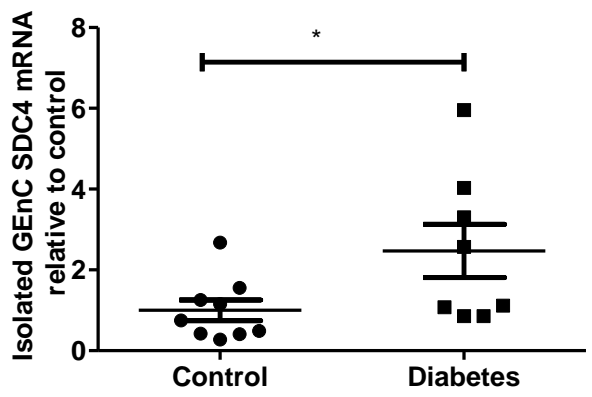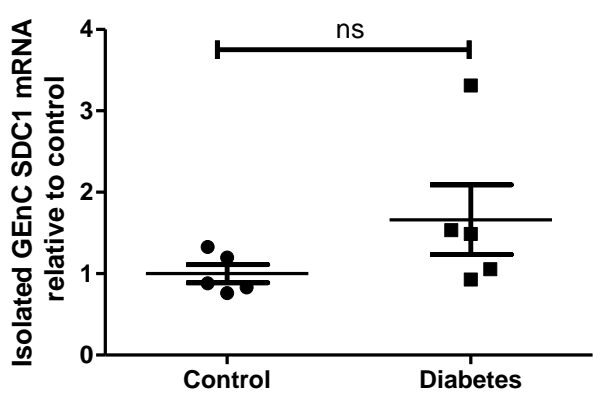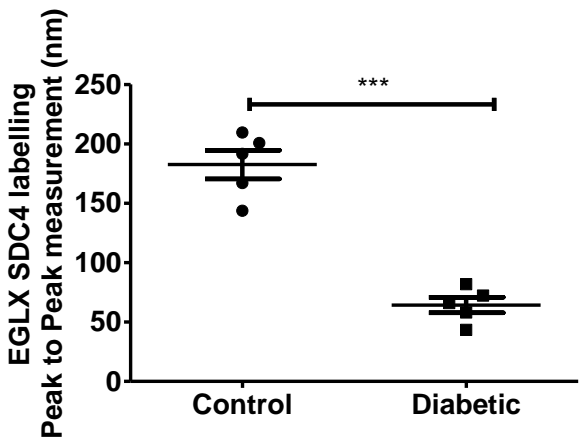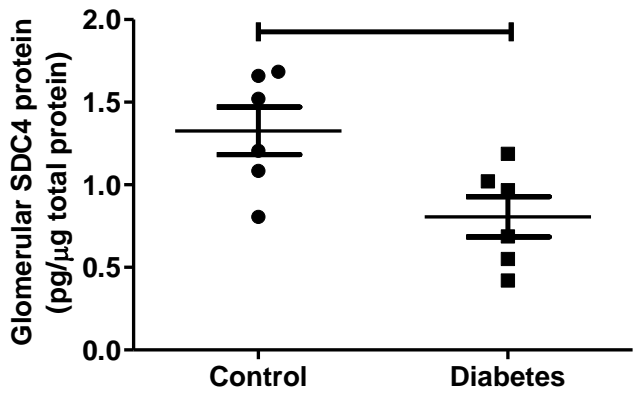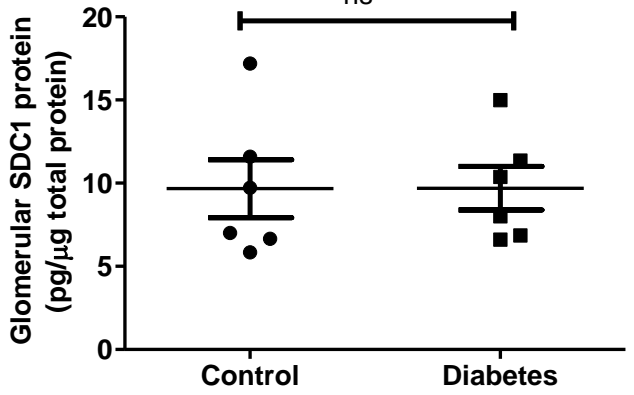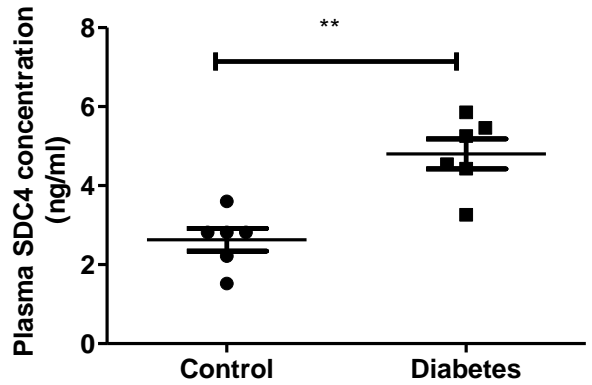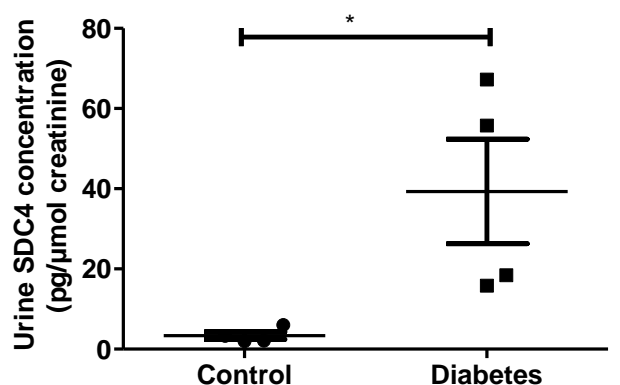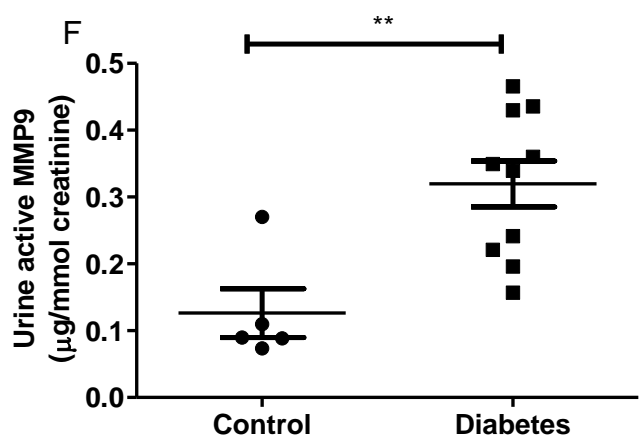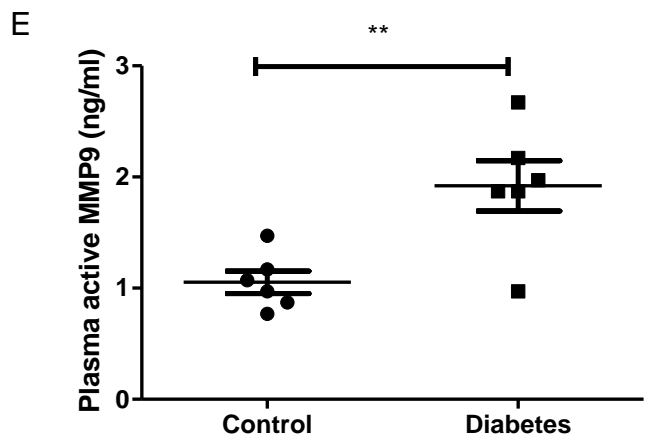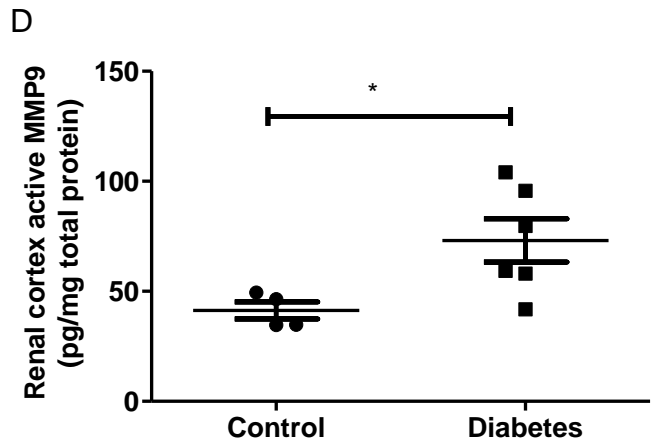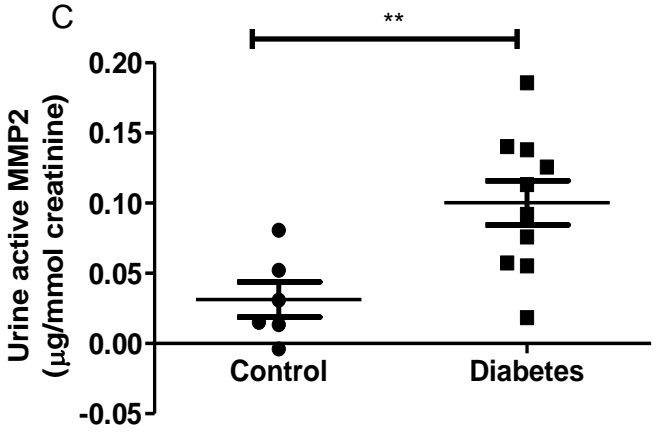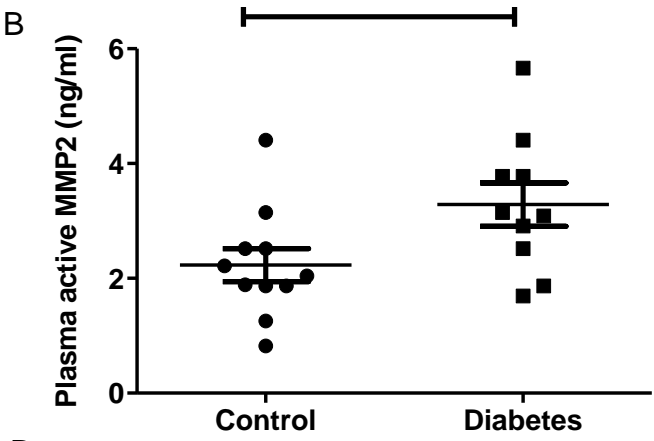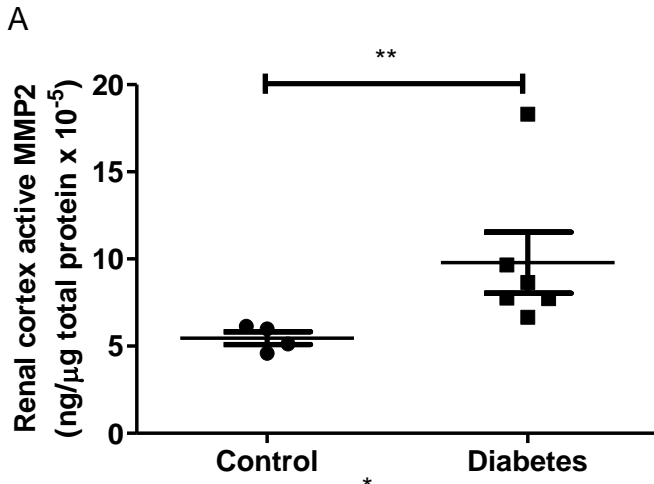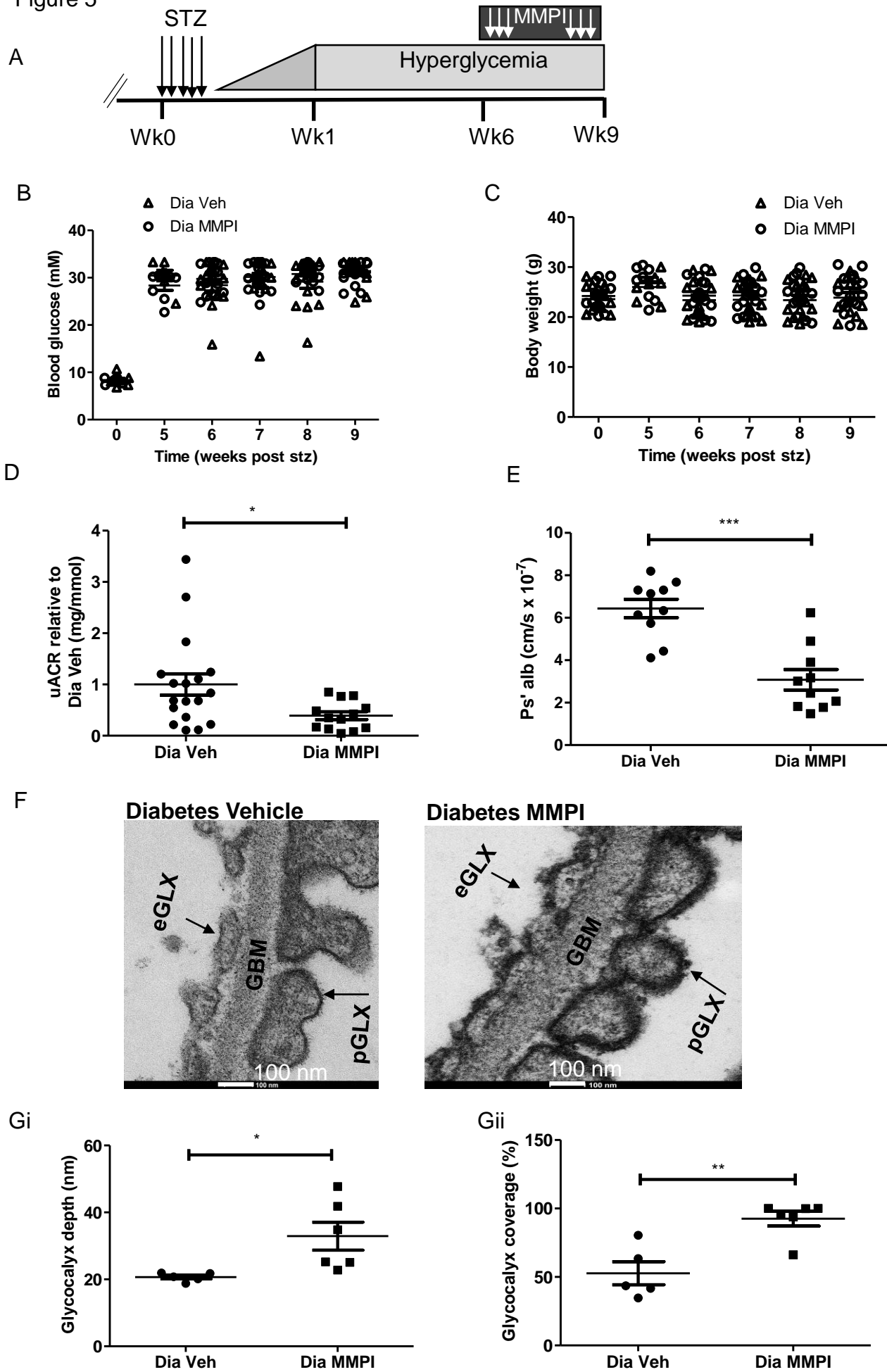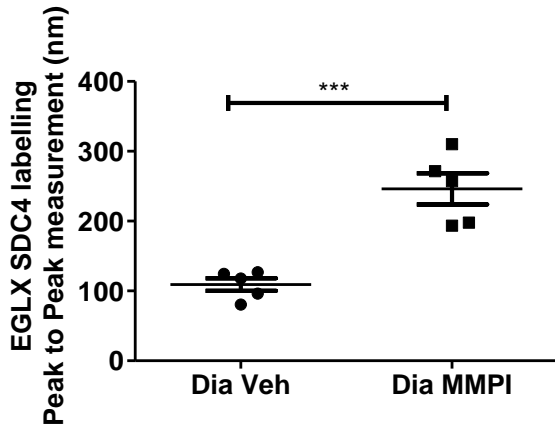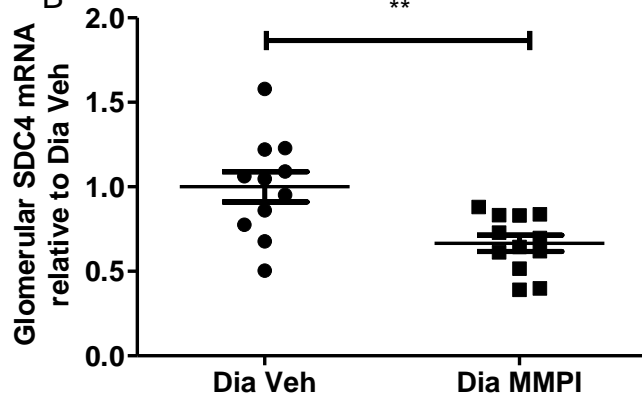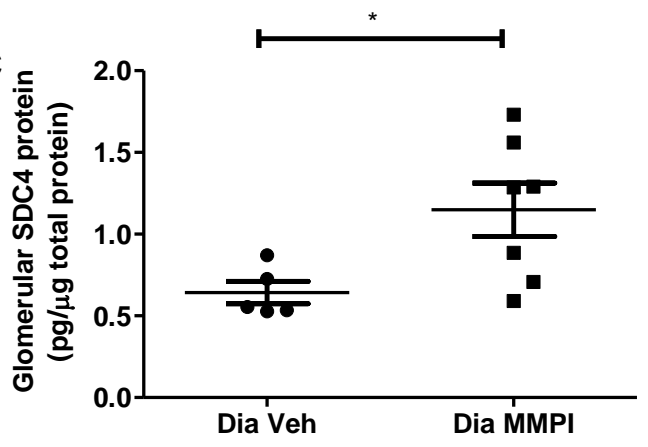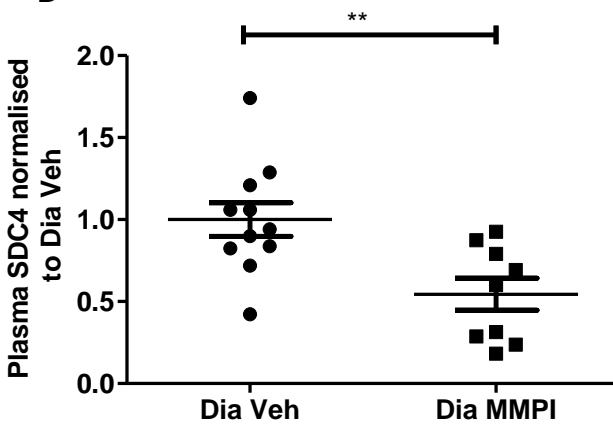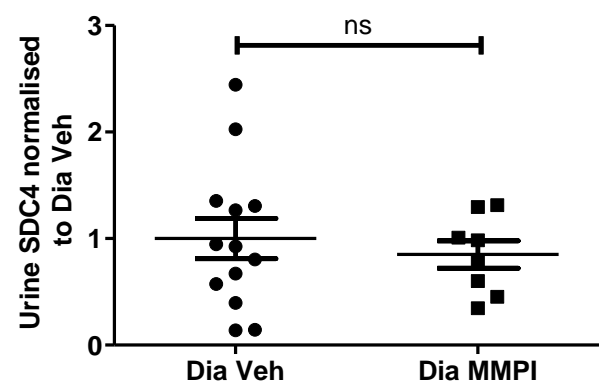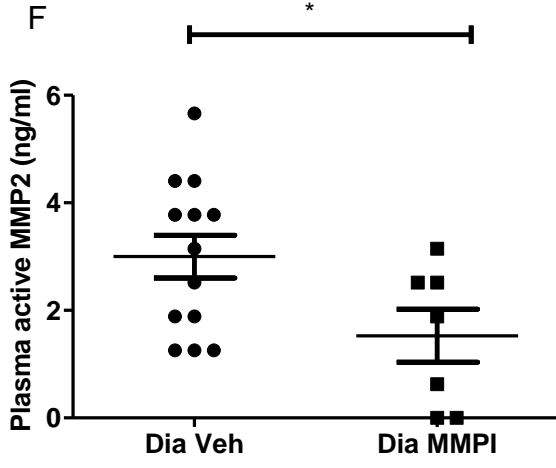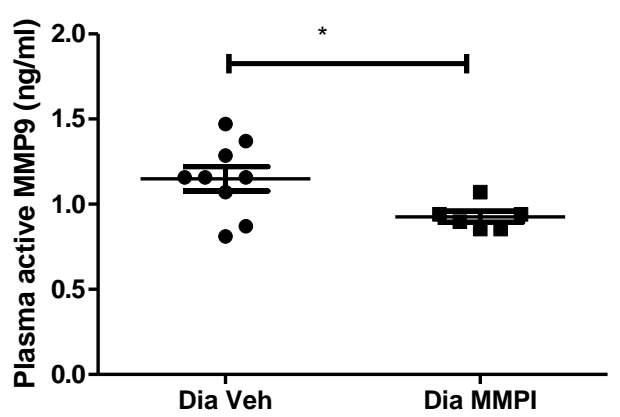
Figure 6

Supplementary Figure 1

Ai
Control — Diabetes

5 μm — pGLX — 5 μm

Aii
pGLX — 200 nm — 200 nm — pGLX

Bi

Glycocalyx depth (Podocyte, nm)

*

Control — Diabetes

Bii

Glycocalyx coverage (Podocyte, %)

ns

Control — Diabetes

C

GBM thickness (nm)

ns

Control — Diabetes

D

Slit diaphragm width (nm)

ns

E

Foot process width (nm)

ns

F

Control   **Diabetes**

G

CTCF

ns
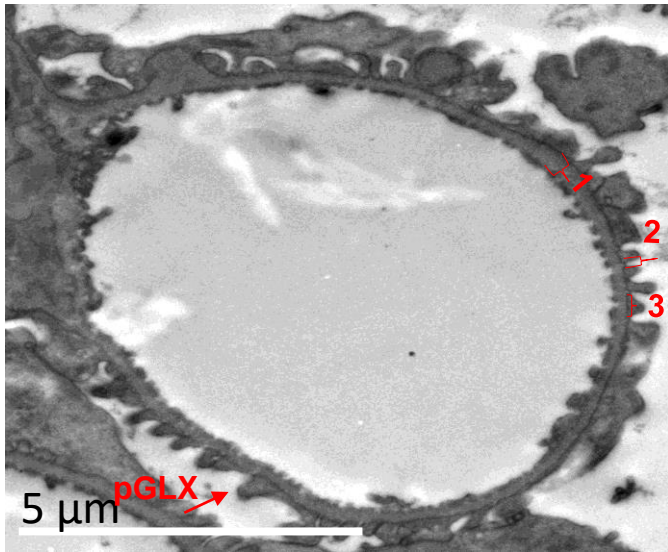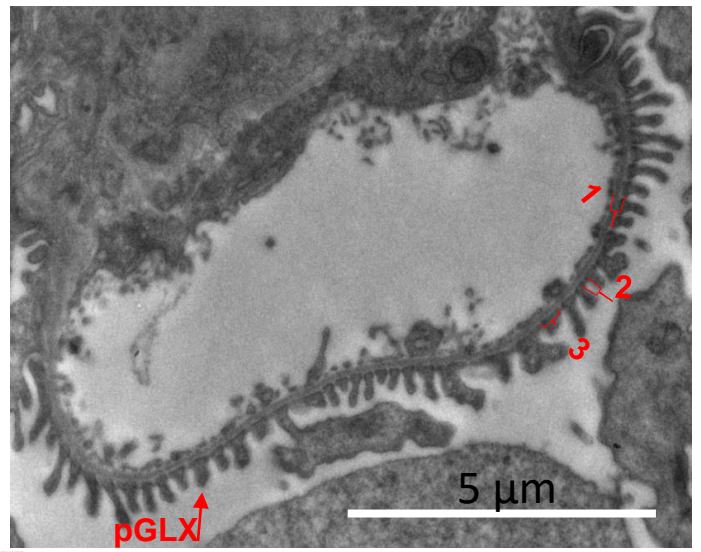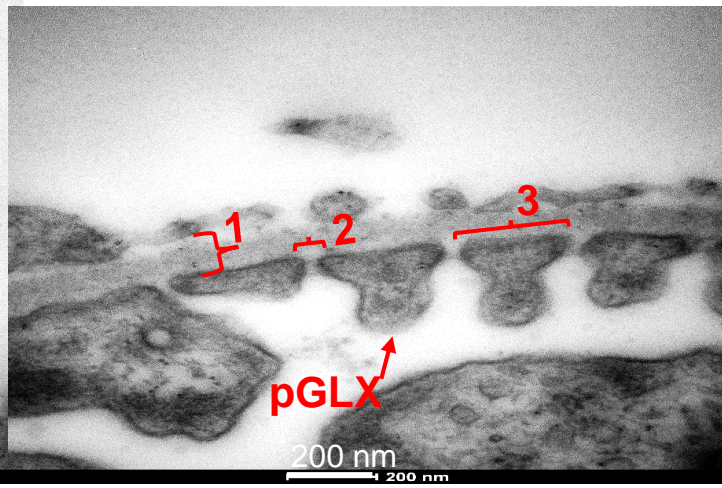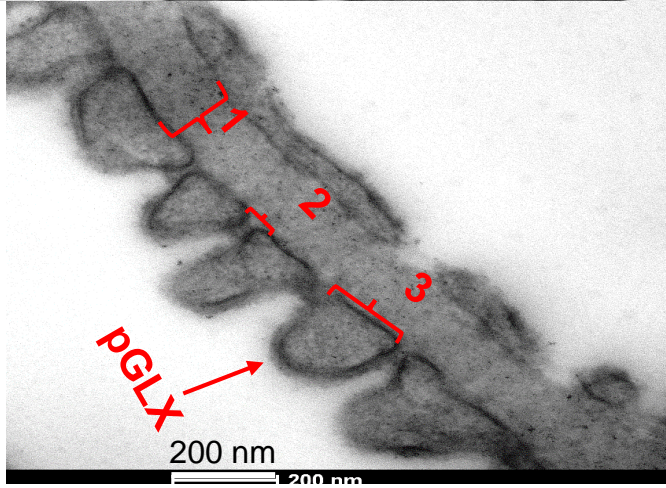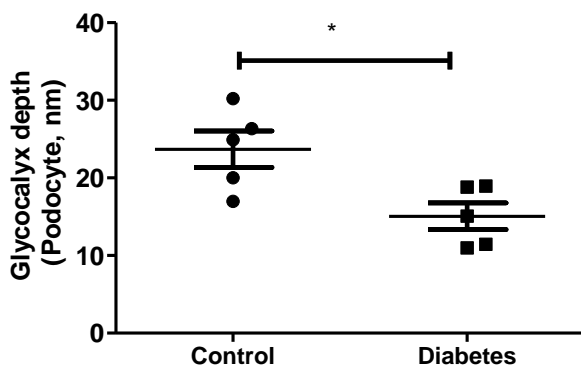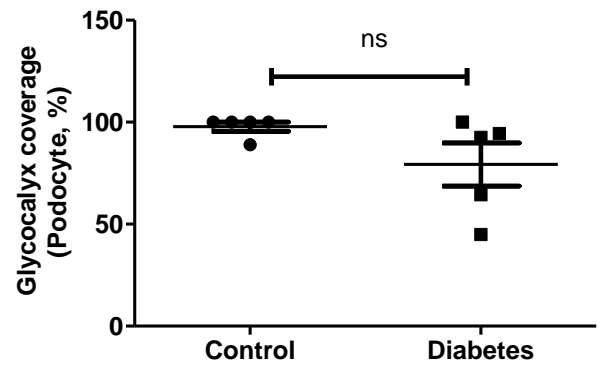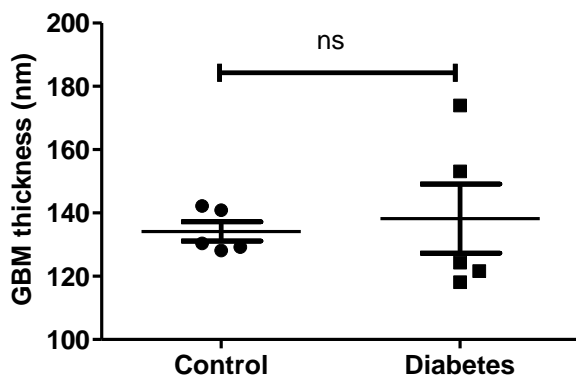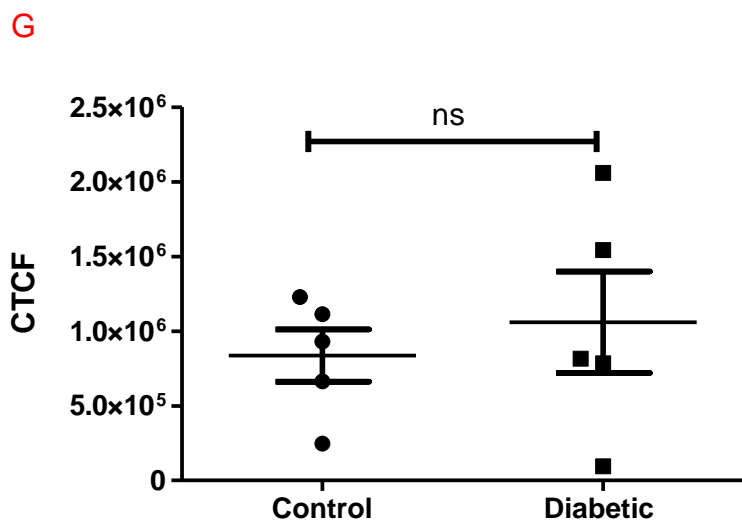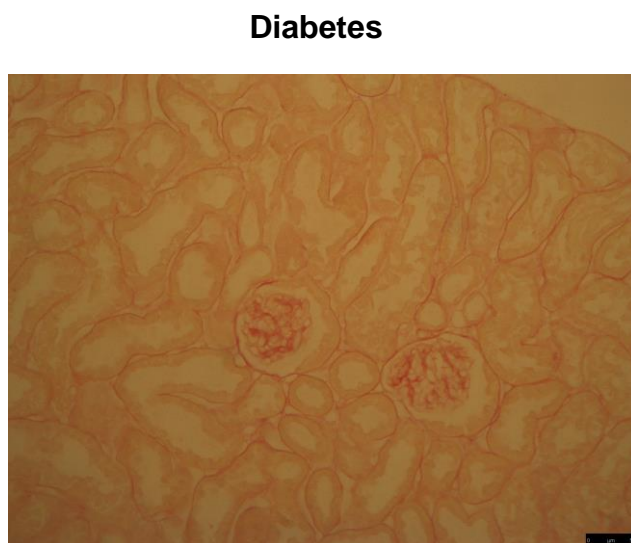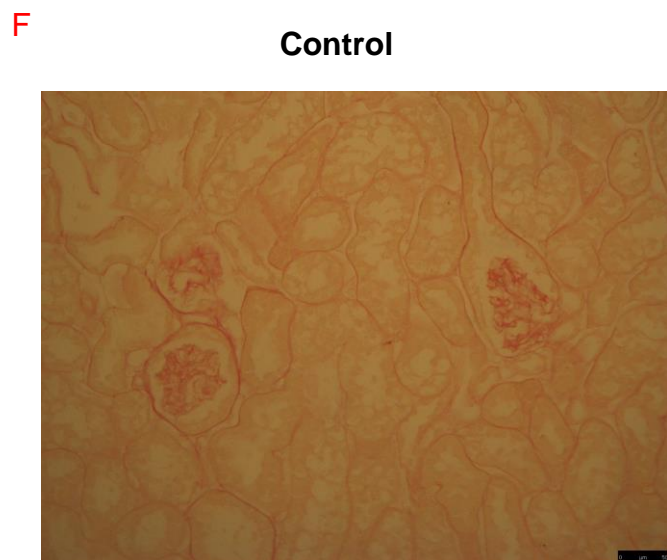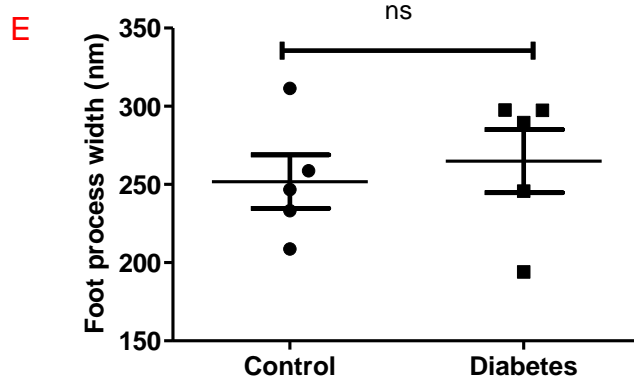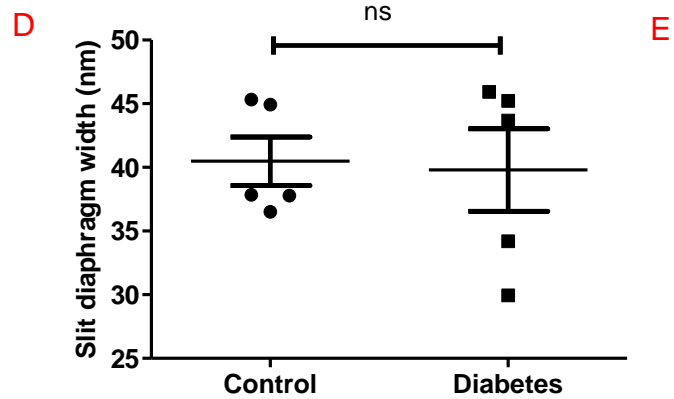
Supplementary Table 1

Class	Name	Symbol
Proteoglycans	Syndecan	SDC 1, 2, 3, 4
	Glypican	GPC 1, 5
	Biglycan	BGN
	Heparan sulfate proteoglycan 2	HSPG2
	Versican	VCAN
	Endothelial cell-specific molecule 1	ESM1
	Decorin	DCN
	Lumican	LUM
Proteoglycan degrading enzymes	Matrix metalloproteinase	MMP 2, 3, 7, 9, 14, 16
	ADAM Metallopeptidase Domain	ADAM 17
	ADAM Metallopeptidase With Thrombospondin Type 1 Motif	ADAMTS 1, 4
HS-synthesizing enzymes	Exostoses	EXT 1, 2
	N-deacetylase/N-sulfotransferase	NDST 1, 2
	Heparan sulfate 2-O-sulfotransferase	HS2ST1
	Heparan sulfate 6-O-sulfotransferase	HS6ST 1, 2
HS-degrading/modifying enzymes	Heparanase	HPSE
	Sulfatase	SULF 1, 2
Chondroitin sulfate-synthesizing enzymes	Chondroitin sulfate N-acetylgalactosaminyltransferase	CSGALNACT 1, 2
	Chondroitin sulfate synthase	CHSY
GAG biosynthesis	Carbohydrate Sulfotransferase	CHST 2, 11
Hyaluronan-synthesizing enzymes	Hyaluronan synthase	HAS 1, 2, 3
Hyaluronan-degrading enzymes	Hyaluronoglucosaminidase 1, 2	HYAL 1, 2
Hyaluronan receptors	Hyaluronan Mediated Motility Receptor	HMMR
	CD44 Molecule (Indian Blood Group)	CD44
Sialic acid-modifying enzymes	Glucosamine (UDP-N-acetyl)-2-epimerase	GNE
	N-Acetylneuraminic acid synthase	NANS
	Sialidase	NEU
Sialoglycoproteins	Endomucin	EMCN
	Podocalyxin-like	PODXL 1, 2
Others	Thrombomodulin	THBD
Housekeeping genes	Glyceraldehyde-3-Phosphate Dehydrogenase	GAPDH
	Eukaryotic 18S rRNA	18S
	Actin, β	ACTB

Supplementary Table 1: List of glycocalyx related genes represented on custom-designed TaqMan qPCR array

Supplementary Table 2

Genes	Expression Suite software	$2^{-\Delta\Delta CT}$ method followed by t test
SDC1	↑2.5 fold, *p= 0.02	↑2.6 fold, **p= 0.002
SDC2	↑1.0 fold, p= 0.80	↑1.1 fold, p=0.82
SDC3	↑2.4 fold, **p= 0.006	↑2.4 fold, **p 0.001
SDC4	↑1.5 fold, *p=0.032	↑1.6 fold, *p 0.039
MMP2	↑6.5 fold, p=0.24	↑8.3 fold, p=0.11
MMP9	↑1.0 fold, p=0.40	↑1.0 fold, p=0.97
MMP14	↑2.2 fold, **p=0.009	↑2.2 fold, **p=0.008

Supplementary Table 2: Two complementary methods were used to analyse the qPCR array data. Expression Suite software and $2^{-\Delta\Delta CT}$ method followed by t test were used to analyse the array data and both methods showed a significant increase in SDC1, 3, 4 and MMP14 mRNA expression amongst other significantly modulated gene expression.

Supplementary Table 3

Genes	Interrogated Sequence		Translated Protein	Exon Boundary	Assay Location	Amplicon Length
SDC1	RefSeq	NM_011519.2	NP_035649.1	2--3	387	131
SDC2	RefSeq	NM_008304.2	NP_032330.1	3--4	833	113
SDC3	RefSeq	NM_011520.3	NP_035650.2	4--5	1293	51
SDC4	RefSeq	NM_011521.2	NP_035651.1	4--5	469	55
MMP2	RefSeq	NM_008610.2	NP_032636.1	2--3	674	62
MMP9	RefSeq	NM_013599.3	NP_038627.1	12--13	2098	76
MMP14	RefSeq	NM_008608.3	NP_032634.3	1--2	376	61
GAPDH	RefSeq	NM_001289726.1	NP_001276655.1	2--3	117	107

Supplementary Table 3: List of primer probes used in this study

Supplementary Figure 2

A

B
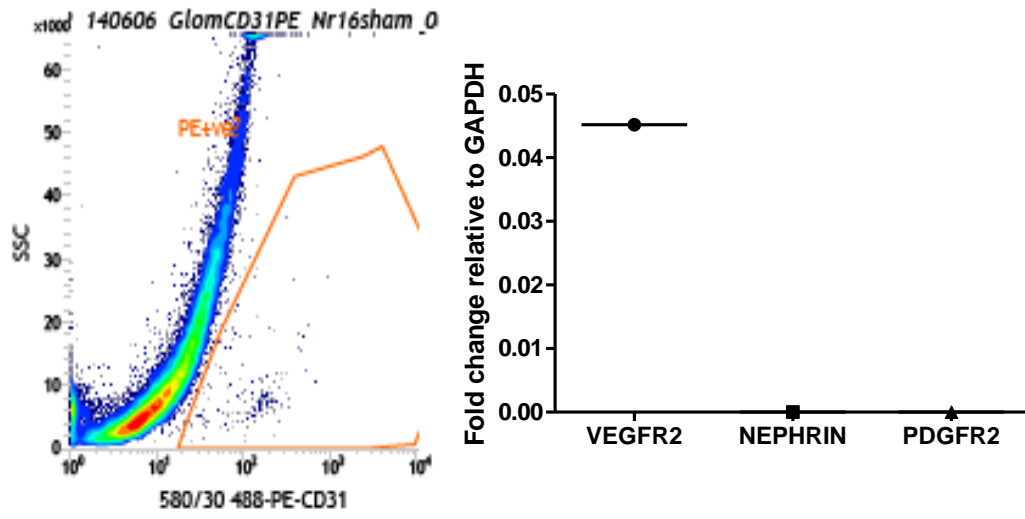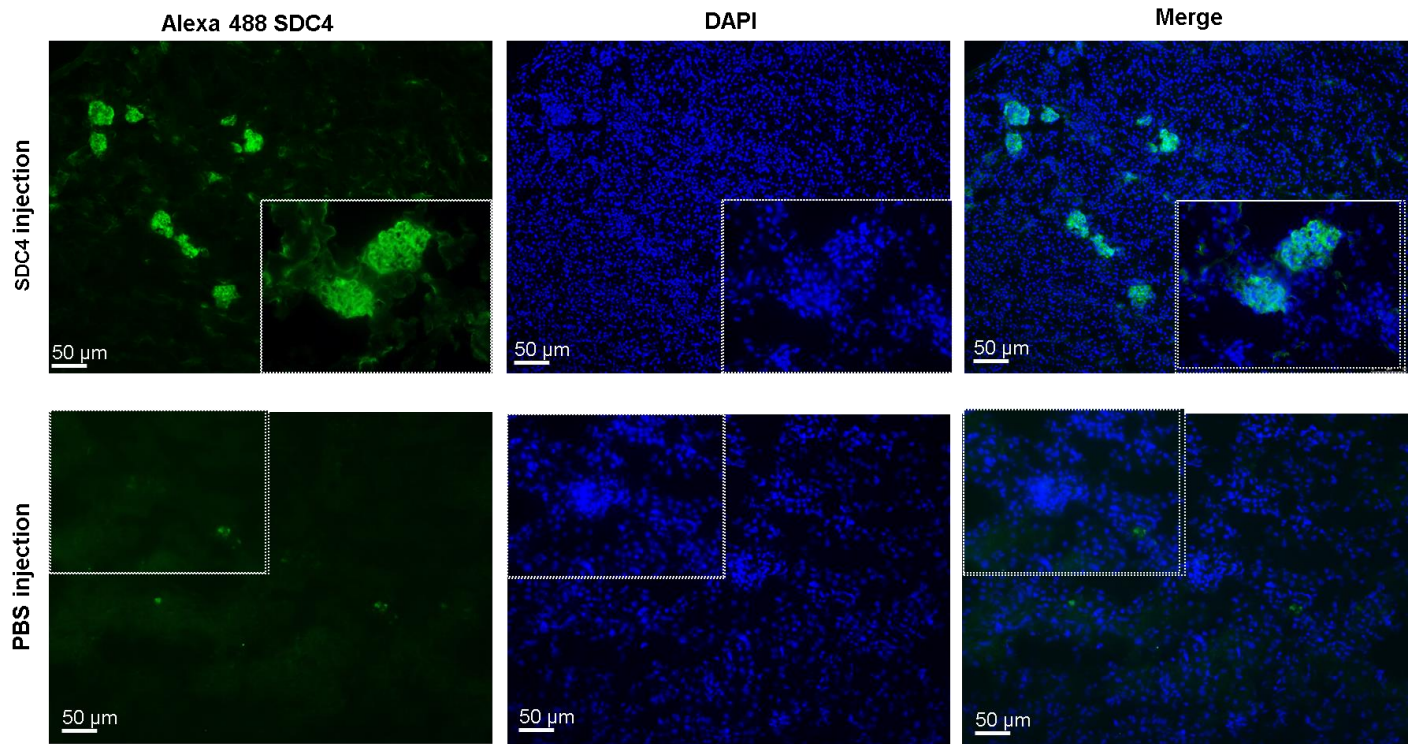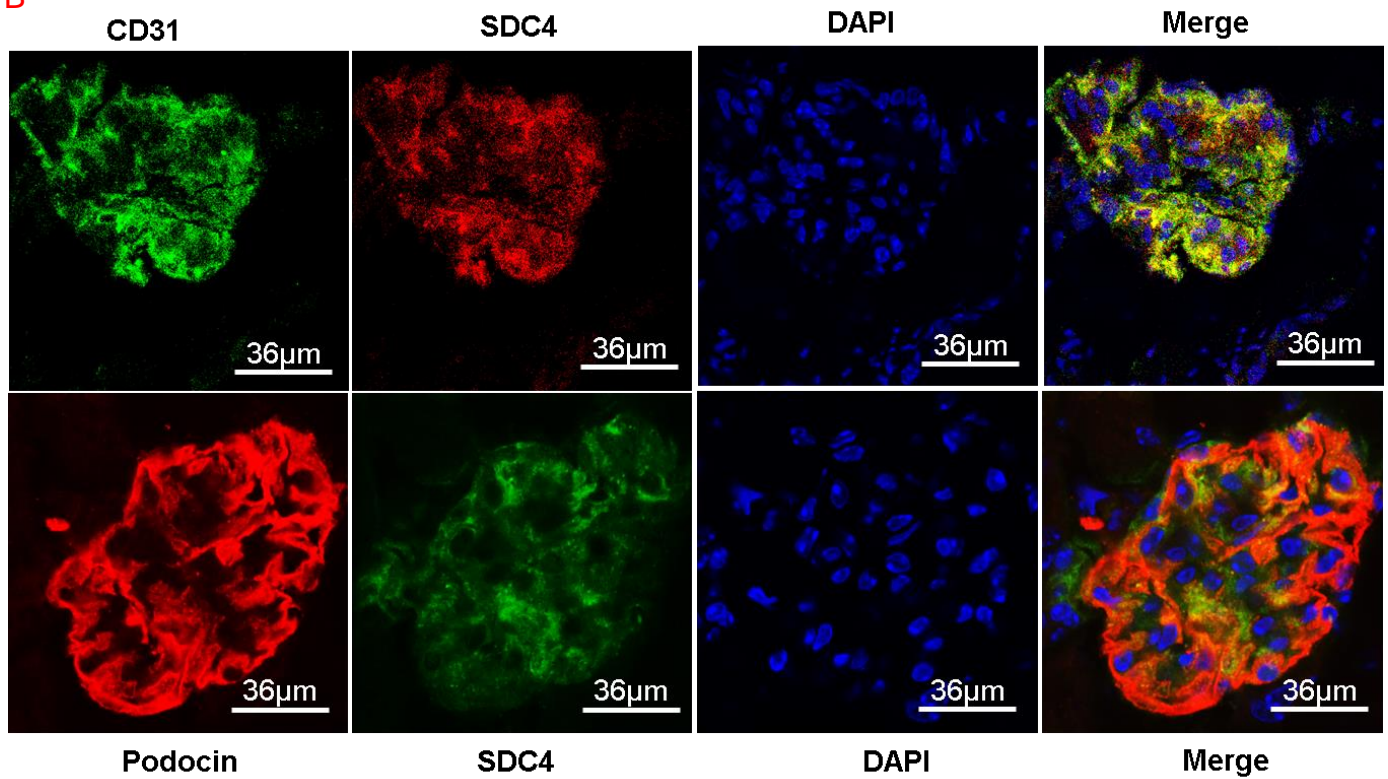
	Albumin (µg/ml)	Creatinine (mmol/L)	ACR (mg/mmol)
Dia Veh	45.9	0.91	50.43956044
Dia Veh	35.6	0.4	89
Dia Veh	6.717853	0.41	16.38500732
Dia Veh	17.3	0.28	61.78571429
Dia Veh	18.8	0.37	50.81081081
Dia Veh	94.2	0.47	200.4255319
Dia Veh	15.9	0.32	49.6875
Dia Veh	48	0.8	60
Dia Veh	15.5	0.39	39.74358974
Dia Veh	71.5	0.64	111.71875
Dia Veh	57.2	0.42	136.1904762
Dia Veh	161	0.8	201.25
Dia Veh	167	0.3	556.6666667
Dia Veh	51.2	0.31	165.1612903
Dia Veh	25.4	0.73	34.79452055
Dia Veh	28.6	0.16	178.75
Dia Veh	4.303508	0.23	18.71090435
Dia Veh	7.112287	0.41	17.34704146
Dia MMPI	16.7	0.42	39.76190476
Dia MMPI	33.6	0.58	57.93103448
Dia MMPI	3.232883	0.26	12.43416538
Dia MMPI	12.9	0.5	25.8
Dia MMPI	16.2	0.45	36
Dia MMPI	4.296473	0.58	7.407712069
Dia MMPI	4.284453	0.34	12.60133235
Dia MMPI	63.3	0.92	68.80434783
Dia MMPI	7.083118	0.33	21.46399394
Dia MMPI	37.4	0.3	124.6666667
Dia MMPI	19.8	0.38	52.10526316
Dia MMPI	24.8	0.98	25.30612245
Dia MMPI	41.4	0.3	138

Supplementary Table 4 shows the absolute values of albumin, creatinine and albumin creatinine ratio from 3 independent experiments carried out on diabetic (Dia) + MMPI or vehicle (Veh) mice.
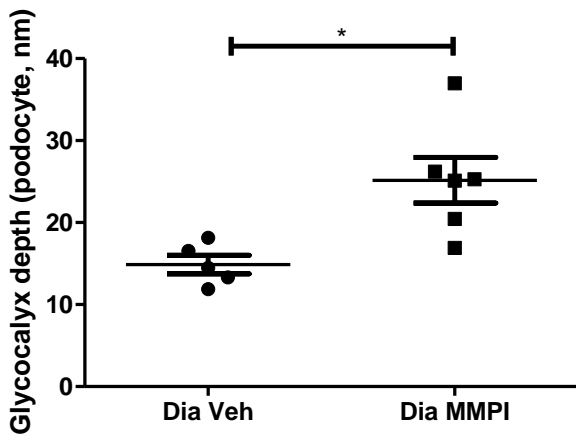
Supplementary Figure 4

Ai

Diabetes Vehicle

Diabetes MMPI
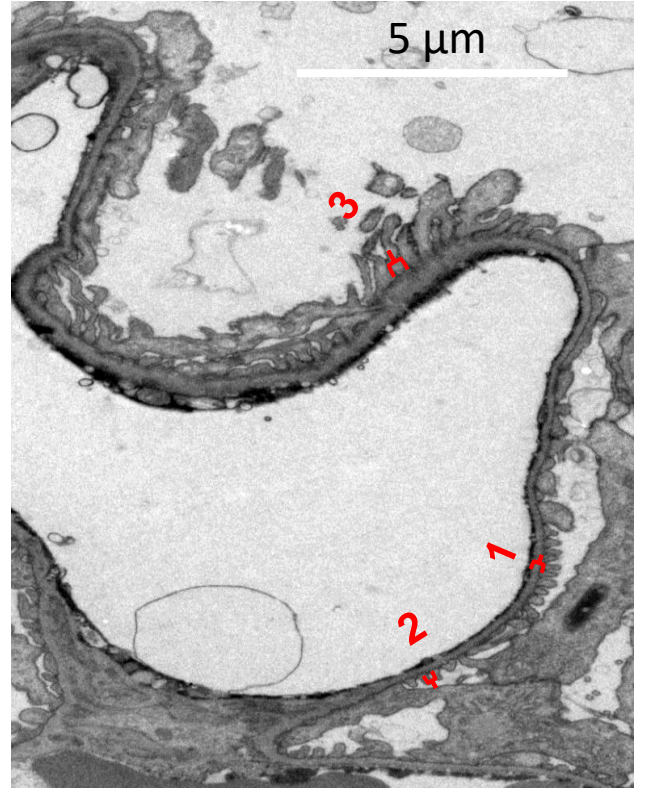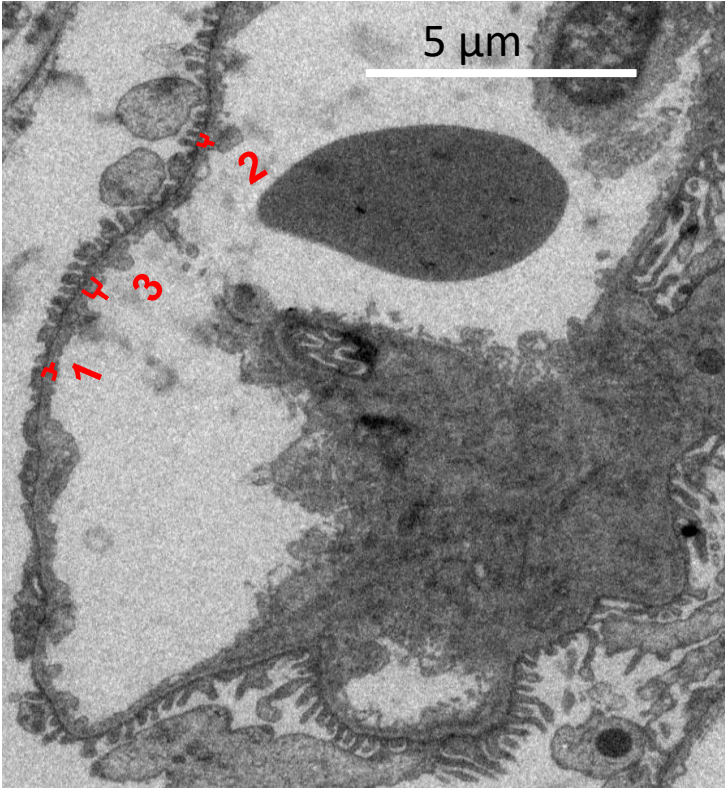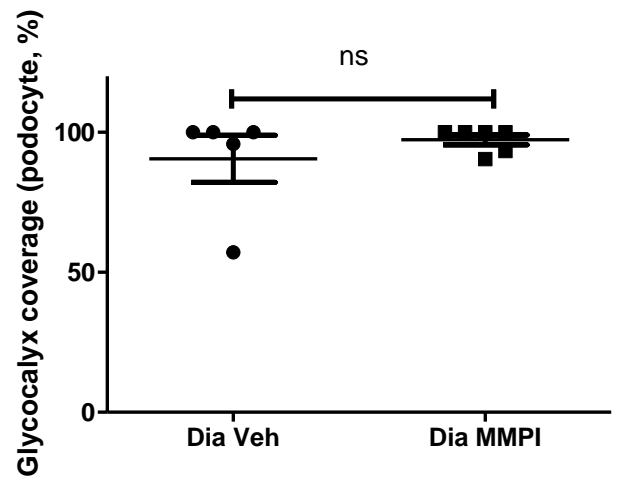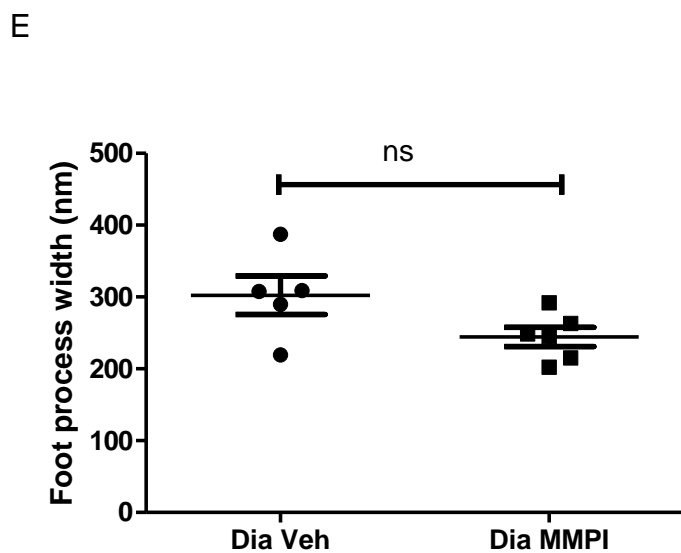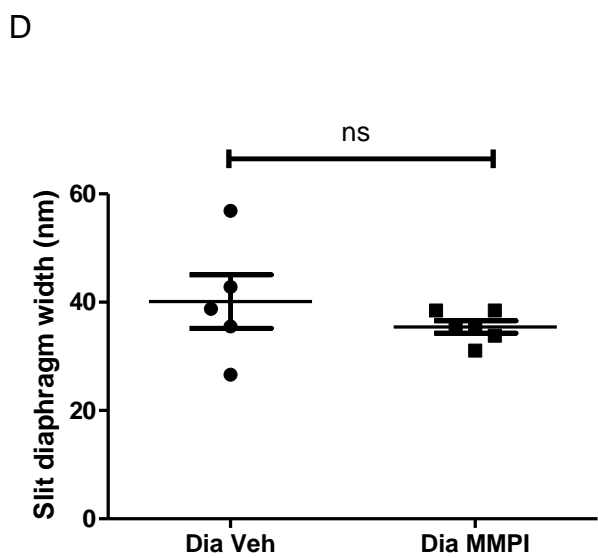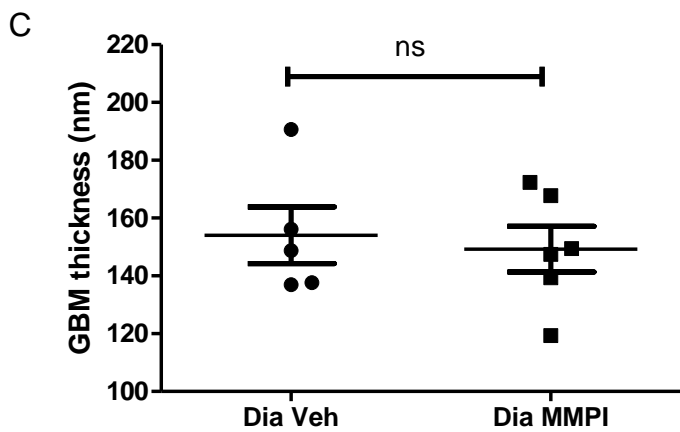

Aii
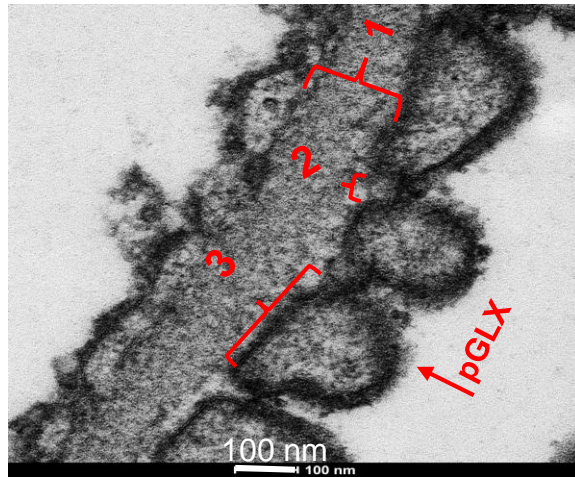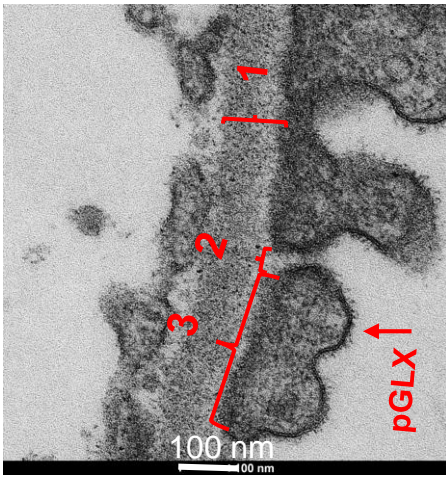
Bi

Bii

Blocking matrix metalloproteinase-mediated syndecan-4 shedding restores the endothelial glycocalyx and glomerular filtration barrier function in early diabetic kidney disease

MMP upregulation and glomerular endothelial glycocalyx syndecan 4 loss are associated with glomerular dysfunction
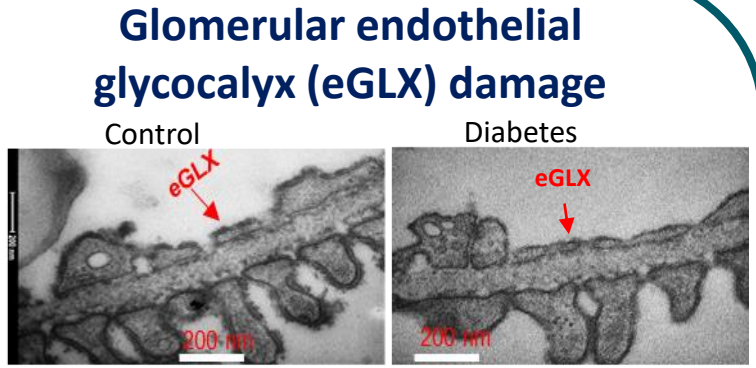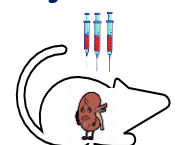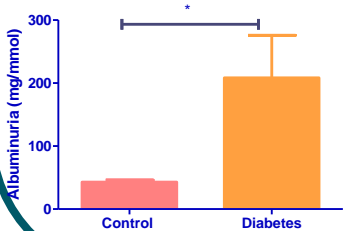
→ Therapeutic treatment with MMP2/9 inhibitor

→ Restores glomerular endothelial glycocalyx syndecan 4 and kidney function

Type 1 diabetes model
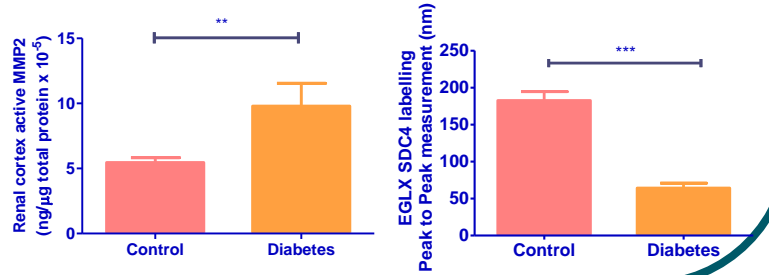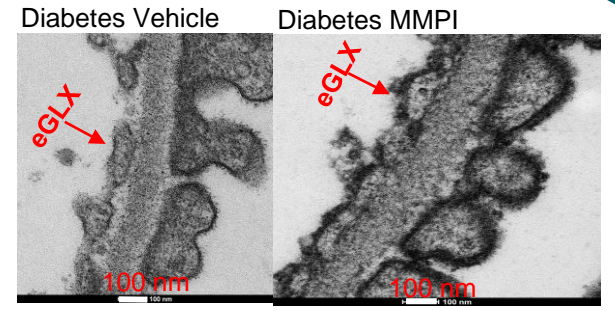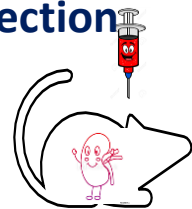Streptozotocin injection

Glomerular endothelial glycocalyx (eGLX) damage

Control / Diabetes — eGLX

Glomerular dysfunction

Albuminuria (mg/mmol) — Control / Diabetes — *

MMP upregulation and eGLX syndecan 4 loss in diabetes

Renal cortex active MMP2 (ng/μg total protein x 10⁻⁵) — Control / Diabetes — **

EGLX SDC4 labelling Peak to Peak measurement (nm) — Control / Diabetes — ***

Streptozotocin injection

MMP2/9 inhibitor injection

Diabetes Vehicle / Diabetes MMPI — eGLX — 100 nm

EGLX syndecan 4

EGLX SDC4 labelling Peak to Peak measurement (nm) — Dia Veh / Dia MMPI — ***

Glomerular dysfunction

Albuminuria (mg/mmol) — Dia Veh / Dia MMPI — *
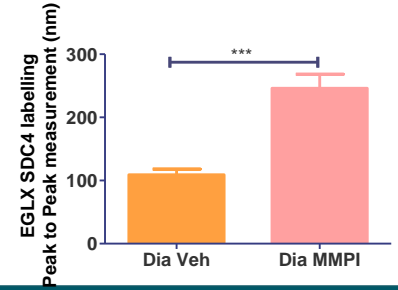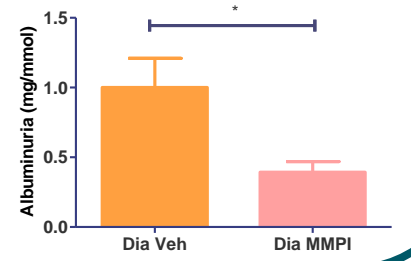
CONCLUSION:
This study confirms the importance of MMPs in endothelial glycocalyx damage and kidney dysfunction in early diabetes and demonstrates that this pathway is amenable to therapeutic intervention.